PB-216 366

FOAM FRACTIONATION WITH REFLUX

Robert Lemlich

Cincinnati University
Cincinnati, Ohio

1 December 1966

DISTRIBUTED BY:

NTIS

National Technical Information Service
U. S. DEPARTMENT OF COMMERCE
5285 Port Royal Road, Springfield Va. 22151

PB 216 366

Privileged Communication

Progress Report

FOAM FRACTIONATION WITH REFLUX

WP-00161

September 1, 1964 through November 30, 1966

Robert Lemlich, Principal Investigator

University of Cincinnati

December 1, 1966

Summary

The theoretical model for foam drainage and overflow, which was developed earlier, was tested in detail against experimental data. This data was gathered from foam fractionation columns, the operation of which included reflux, no reflux, pool feed, and foam feed. The test yielded good agreement. The average deviation of theory from experiment for foam overflow rate was only 26% over a 1000-fold range.

The theory was also tested against experimental data for stationary foam draining at steady state. This too yielded good agreement.

The theoretical model was then extended to stationary foam in unsteady state drainage by combining it with a differential mass balance and suitable boundary conditions. A comparison of theoretical prediction with experimental measurement indicated that the effect of bubble coalescence in the foam can be very important in this situation.

Six publications have appeared and one more is in review.

Reproduced by
NATIONAL TECHNICAL
INFORMATION SERVICE
U S Department of Commerce
Springfield VA 22151

CONTENTS

	Page
List of seven publications	3
Other contributions	4
Staff	4
Six publications in print	Insert
Publication under review	5
Additional work	25

Note: In each section of this report, the equations, figures, and bibliographical references are numbered independently of any other section.

PUBLICATIONS

1. Leonard, R. A. and Lemlich, R., "A Study of Interstitial Liquid Flow in Foam. Part I: Theoretical Model, and Application to Foam Fractionation", Am. Inst. Chem. Engrs. Jour., 11:18 (1965).

2. Leonard, R. A. and Lemlich, R., "A Study of Interstitial Liquid Flow in Foam. Part II: Experimental Verification and Observations", Am. Inst. Chem. Engrs. Jour., 11:25 (1965).

3. Leonard, R. A. and Lemlich, R., Communication: "Laminar Longitudinal Flow between Close-Packed Cylinders", Chem. Eng. Sci. 20:790 (1965).

4. Dorman, D. C. and Lemlich, R., "Separation of Mixtures by Nonfoaming Bubble Fractionation", Nature 207:145 (1965).

5. Harper, D. O. and Lemlich, R., "Bubble and Foam Fractionation Combined", Ind. Eng. Chem. Process Design and Development Quart., 4:13 (1965).

6. Fanlo, S. and Lemlich, R., "Predicting the Performance of Foam Fractionation Columns", A.I.Ch.E.-I.Chem.E. Symposium Series (London: Instn. Chem. Engrs.) No. 9, 75 (1965).

7. Shih, F. S. and Lemlich, R., "A Study of Interstitial Liquid Flow in Foam. Part III: Test of Theory", Am. Inst. Chem. Engrs. Jour., in review.

OTHER CONTRIBUTIONS

The Principal Investigator presented the paper entitled "Predicting the Performance of Foam Fractionation Columns" at the joint meeting of the Institution of Chemical Engineers (British) and the American Institute of Chemical Engineers which was held in London during June 1965.

In addition, the Principal Investigator spoke on the subject of foam fractionation at the Free Forum of the annual A.I.Ch.E. meeting in Boston during December 1964, at a Gordon Research Conference in New London (New Hampshire) during August 1966, and at several universities.

STAFF

Name	Title	Appointment	Effort
Lemlich, R.	Principal Investigator	9/1/64 - 11/30/66	25%
Dorson, D. C.	Assistant	9/1/64 - 6/30/65	20%
Drott, D. W.	Assistant	1/1/66 - 5/31/66	50%
"	"	6/1/66 - 8/31/66	100%
Shih, F. S.	Assistant	9/1/64 - 12/31/64	50%
"	"	6/1/65 - 8/31/65	50%
"	"	9/1/65 - 11/30/66	100%

Reprinted From . . .

A.I.Ch.E.
JOURNAL

A STUDY OF INTERSTITIAL LIQUID FLOW IN FOAM

PART I

Theoretical Model and Application to Foam Fractionation

PART II

Experimental Verification and Observations

Ralph A. Leonard and Robert Lemlich

VOL. 11, NO. 1 JANUARY 1965 PAGES 18-28

A Study of Interstitial Liquid Flow in Foam

RALPH A. LEONARD and ROBERT LEMLICH

University of Cincinnati, Cincinnati, Ohio

Part I. Theoretical Model and Application to Foam Fractionation

A theoretical model for interstitial liquid flow in a stationary or moving foam was devised by relating the physical structure of the foam to the physical properties of the surfactant and the foam movement. This was accomplished through a differential momentum balance within a typical capillary (Plateau border) of noncircular cross section with finite surface viscosity at its boundaries. Velocity profiles were then calculated and integrated numerically for the randomly oriented capillaries so as to obtain the overall liquid flow through the foam in terms of the pertinent variables. Results are presented in a form suitable for estimating concentrations and flow rates of product and waste streams in foam fractionation.

In recent years there has appeared a revival of interest in the potentialities of separating mixtures by foam fractionation. This technique of separation is based on the adsorption of a solute at the surface of bubbles formed by sparging a liquid mixture. These bubbles rise to form a foam which carries solute off overhead. A foam fractionation column can be operated as a refluxing enricher (*16*), a stripper (*17*), or both (*11*). Applications include water renovation (*13, 15*), radioactive effluent purification (*6, 26*), and protein separation (*25*). An extensive review of the literature has recently appeared (*24*).

Some introductory analyses have been presented for the operation of foam fractionation columns (*5, 24*). These analyses show the quantitative role played by surface adsorption. However, they are incomplete in that they do not provide an independent relationship for foam density or for the flow rate of foam overhead. This lack, of course, stems from the complicated nature of foam drainage, especially in a moving column of foam which is constantly being formed at one end and removed at the other.

Accordingly, the present investigation was aimed at devising and testing a more complete model which would include the interstitial liquid flow in the foam. The theoretical development is presented here, together with a design procedure. Experimental confirmation is presented in Part II of this paper. Part II also includes the complete notation for both Parts I and II.

Figure 1 shows a typical foam fractionation column (in this case without external reflux) operating under steady state conditions. By overall balance

$$F = D + W \tag{1}$$

Also, by material balance for a single surfactant

$$C_F F = C_D D + C_W W \tag{2}$$

The surfactant passing overhead, namely $C_D D$, can be divided into two parts so as to represent the physical picture more closely (*5*). The first part is the surfactant adsorbed at the bubble surfaces. This amounts to $6G\Gamma/d_m$. The second part is that in the interstitial liquid $C_L D$. Substitution in Equation (2) yields

$$C_F F = C_L D + \frac{6G}{d_m}\Gamma + C_W W \tag{3}$$

In a typical situation, F, G, and C_F might be the given independent variables. Average bubble diameter d_m would depend on G, C_W, and the sparger. With the feed inlet several diameters or more above the liquid pool, the rising foam would be well rinsed with downcoming feed so that C_L should closely approach C_F if there is no coalescence [breakage] of bubbles in the foam within the column. This pinch in concentration occurs at the level of the feed rather than at the bottom because in the column section below the feed point the rate of liquid downflow exceeds the rate of upflow.

Γ can be measured independently in a standard recirculating separator (*5*) or, in certain cases, estimated from surface tension measurements via the Gibbs adsorption equation (*7, 22*). It is fairly constant over a wide range of concentration.

All this effectively leaves the two Equations (1) and (3) with three unknown variables, namely C_W, W, and D. The present study involves the development of a theory for foam drainage which can be used to predict D independently of Equations (1) and (3), thus permitting a more complete solution to the entire problem of foam fractionation.

FOAM STRUCTURE

Foams can be divided into two extreme types (*1, 19*). These are wet* foams, or kugelschaums, with spherical bubbles and dry† foams, or polyederschaums, with polyhedral bubbles. Except for very small bubble sizes or very viscous liquids, kugelschaums do not normally exist at distances higher than one bubble diameter above the liquid pool. Thus, polyederschaums represent the more usual situation and so will be considered here as forming the basic foam structure.

For a polyederschaum of reasonably uniform bubble size, the foam structure can be approximated by bubbles in the shape of regular dodecahedra (*1, 2, 19*). The bubbles are packed so that their pentagonal faces fit together symmetrically three at a time to form a line, with a dihedral angle of approximately 120 deg. between faces. These lines, in turn, fit together symmetrically four at a time with an angle of approximately 109 deg. between lines.

Of course the packing fit is not perfect. With identical regular dodecahedra, geometric considerations show that

Ralph A. Leonard is with the E. I. du Pont de Nemours and Company, Inc., Wilmington, Delaware.

* Meaning high liquid content.

† Meaning low liquid content.

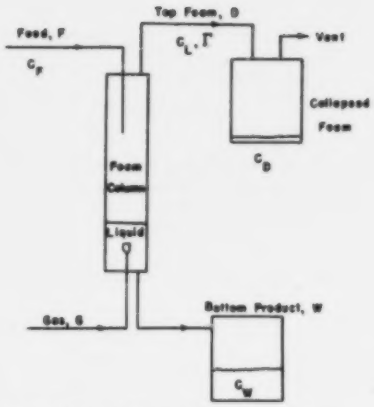

Fig. 1. A typical foam fractionation column.

3% of the space remains unfilled. This contributes to some distortion. However, the picture is fairly good and accordingly is used in the model developed here.

The "unfilled" space between bubbles is actually filled with the interstitial liquid. Most of the liquid is in the aforementioned lines which are really capillaries known as Plateau borders (*2*). The remaining liquid is in the films that make up the bubble faces.

Figure 2 shows a Plateau border (abbreviated hereafter as PB) in cross section. The shaded area is in sixfold symmetry within a PB.

Flow through a PB is essentially axial. Thus there is little pressure gradient within the PB in the radial or angular directions. Therefore, the pressure difference across the curved PB-gas boundary such as DWE should be virtually uniform from point to point along the boundary. This pressure difference between the liquid in the PB and the gas in the bubble proper is given by the equation of Laplace and Young (*1*) as

$$p_{vst} - p_{lq} = \frac{\gamma}{r_s} \tag{4}$$

Since γ is uniform, r_s is uniform. Accordingly, boundary DWE is represented as a circular arc. It should be noted that r_s is the radius of curvature of the PB-gas boundary and not the radius of the bubble.

Since each bubble face is essentially flat, there is virtually no corresponding pressure difference between the liquid in a film and the gas in the bubble. Therefore, there must be a sharp pressure gradient within the liquid at the PB-film border, such as at point A of Figure 2. The existence of this sharp gradient has been defended and used to explain marginal regeneration (*21*).

From geometric considerations

$$A_{PB} = \left(3\sqrt{3} - \frac{3}{2}\pi\right)a^2 + 3at + \frac{\sqrt{3}}{4}t^2 \tag{5}$$

Since $a >> t$ normally, and $r_s = a\sqrt{3}$, Equation (5) reduces to Equation (6):

$$A_{PB} = 0.1612\ r_s^2 + 1.732\ r_s t \tag{6}$$

Also by geometry, Equation (7) gives the packing factor P which is the total length of PBs per unit height of column, and Equation (8) gives the liquid to gas ratio in the foam:

$$P = \frac{60A_{col}}{2.445\ \pi d_m^2 (1 + V_L/V_G)} \tag{7}$$

$$\frac{V_L}{V_G} = \frac{60A_{PB}}{2.445\pi d_m^2} + \frac{3t}{d_m} \tag{8}$$

The volumetric density of the foam, $\mathcal{D} = 1 - \epsilon$, is

$$\mathcal{D} = \frac{V_L/V_G}{1 + V_L/V_G} \tag{9}$$

The orientation of a PB in space, without regard to the particular bubble with which it is associated, is taken as being random. This follows from the large number of bubbles present in the foam and the absence of any known factor which would favor one orientation over another.

Foam drainage occurs primarily through the interconnecting PB network (*19*). In other words, each film drains into its own bounding PBs and, at steady state, does not transmit the drainage of other films (*21*).

The liquid-gas boundaries, such as *FDWEG* of Figure 2*b*, exhibit a resistance to shear quite apart from that associated directly with the viscosity of the interstitial liquid. The corresponding physical property for this phenomenon has been termed *surface viscosity*. It is defined as the shearing force per unit length in the surface, divided by the resulting velocity gradient in the surface. This can be compared with the familiar bulk viscosity which of course is the shearing force per unit surface within the bulk divided by the velocity gradient in the bulk.

Surface viscosity is attributed to the surfactant which concentrates at the interface (*1, 8*). It is known to affect drainage (*8, 22*).

It appears that earlier theoretical models for foam drainage are limited in three ways by their simplifying hypotheses of interstitial flow through channels that are vertical, with rigid walls, and of either substantially circular (*10, 20*) or parallel plane (*4, 9, 14, 23*) cross section.

FLOW THROUGH AN INDIVIDUAL PLATEAU BORDER

In view of the sixfold symmetry of the PB cross section as illustrated in Figure 2*b*, a solution need be obtained only for the shaded region *ADWO* in order to provide a complete velocity profile for flow through a PB. This shaded region is conveniently bounded by cylindrical coordinates about point *P* as origin, except for the line *AO* across which mirror symmetry applies.

The equation of motion in cylindrical form (*3*) for a Newtonian fluid with constant ρ and μ flowing in the axial

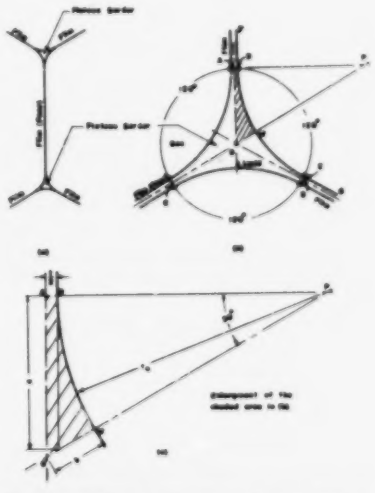

Fig. 2. A Plateau border shown in cross section.

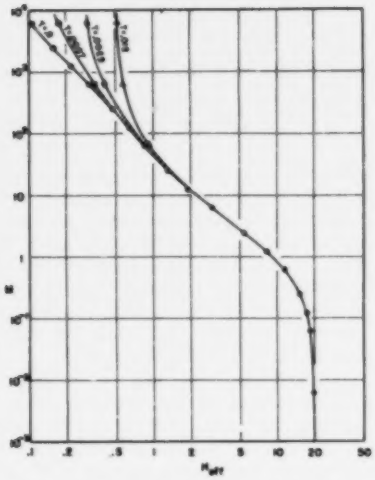

Fig. 3. Dimensionless relationship for flow through a Plateau border.

z direction is

$$\rho\left[\frac{\partial v_z}{\partial \tau}+v_r\frac{\partial v_z}{\partial r}+\frac{v_\theta}{r}\frac{\partial v_z}{\partial \theta}+v_z\frac{\partial v_z}{\partial z}\right]=\frac{-\partial p_{1a}}{\partial z}+$$

$$\mu\left[\frac{1}{r}\frac{\partial}{\partial r}\left(r\frac{\partial v_z}{\partial r}\right)+\frac{1}{r^2}\frac{\partial^2 v_z}{\partial \theta^2}+\frac{\partial^2 v_z}{\partial z^2}\right]+\rho g_z \quad (10)$$

It can be shown that $\partial v_z/\partial \tau$, v_r, v_θ, $\partial v_z/\partial z$, and $\partial^2 v_z/\partial z^2$ are negligible, and $\partial p_{1a}/\partial z << \rho g_z$ so that the quantity $(\rho g_z - \partial p_{1a}/\partial z)$ is essentially constant for a given z orientation relative to the earth. Details of this and other aspects of the entire investigation have been placed on file (*17*).

The terms g_{zzz} and h_{zzz} are now introduced and defined by Equations (11) and (12):

$$g_{zzz}=g_z-\frac{1}{\rho}\frac{\partial p_{1a}}{\partial z} \quad (11)$$

$$h_{zzz}=\frac{\rho g_{zzz}}{\mu} \quad (12)$$

Combining with the above one gets

$$\frac{1}{r}\frac{\partial}{\partial r}\left(r\frac{\partial v_z}{\partial r}\right)+\frac{1}{r^2}\frac{\partial^2 v_z}{\partial \theta^2}=-h_{zzz} \quad (13)$$

where h_{zzz} is constant.

The solution to Equation (13) was obtained through a finite difference approach with fifty-three nodal points. This yielded a matric equation which in turn was solved by means of Crout's reduction (*12*) on an IBM-1620 digital computer. The boundary conditions are those of mirror symmetry at line *OW* of Figure 2 and mirror symmetry at line *OA*. At the PB-gas interface, namely curve *DW*, the boundary condition is that of momentum transfer to a surface with Newtonian surface viscosity μ_s. This gives $\frac{\partial^2 v_z}{\partial \theta^2}=\frac{-\mu r_c^2}{\mu_s}\frac{\partial v_z}{\partial r}$ at the interface. Elements of this boundary surface move perpendicularly to the PB cross section. For reasons discussed later, point *A* is conveniently selected as the datum so that v_z at that point is zero.

Fig. 4. Lines of constant dimensionless velocity for flow through a Plateau border bounded by rigid interfaces. M = 0 and T = 0.

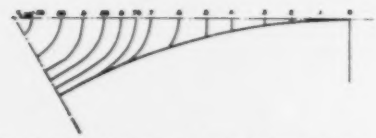

Fig. 5. Lines of constant dimensionless velocity for flow through a Plateau border bounded by interfaces of a moderate surface viscosity. M = 2.48 and T = 0.

The solution for the velocity profile is presented in terms of dimensionless groups defined as follows:

$$H_{zzz}=\frac{h_{zzz}A_{PB}}{v_{z,\max}} \quad (14)$$

$$V_z=\frac{v_z}{v_{z,\max}} \quad (15)$$

$$M=\frac{\mu r_c}{\mu_s} \quad (16)$$

$$T=\frac{t}{r_c} \quad (17)$$

H_{zzz} is a function of M and at high M values is also a function of T. This is shown in Figure 3.* V_z is a function of M and location in the PB, and also a weak function of T. Figures 4, 5, and 6 show lines of constant velocity in a PB cross section for three different cases. In Figure 4 the surface viscosity is very high relative to μr_c so that $M = 0$ and the bounding surfaces are rigid.† In Figure 5 the surface viscosity contributes about equally with μr_c in determining the flow pattern. In Figure 6 M is large, which means the surface viscosity is low relative to μr_c, and so μ_s is the major factor in determining the flow pattern.

Of course, these profiles are restricted to laminar flow. However the experimental results show that flow in the PBs is well within the laminar regime.

PB end effects are neglected, since the PB is relatively long and thin; that is, the ratio E/a is large.

By means of the computer, the velocity profiles were integrated numerically over the cross-sectional area of a PB to yield the volumetric flow rates through an individual PB for various conditions.

In practice p_{1a} cannot be easily measured since it is within a PB. This difficulty can be circumvented by differentiating Equation (4) with respect to z and by com-

* The points shown in Figures 3, 8, 9, and 10 are the individual values which were computed from theory in order to establish the curves.

† This case is of special interest quite apart from the present study in foam, as it is identical with the situation for longitudinal laminar flow along (between) close-packed rigid cylinders (*18*).

Fig. 6. Lines of constant dimensionless velocity for flow through a Plateau border bounded by interfaces of a very low surface viscosity. M = 61.9 and T = 0.

bining with Equation (11) to give Equation (18):

$$g_{eff} = g_c - \frac{1}{\rho}\frac{dp_{net}}{dz} - \frac{\gamma}{\rho r_c^2}\frac{dr_c}{dz} \qquad (18)$$

In all of the foregoing, velocities are relative to an observer located at the PB-film border such as at point A of Figure 2. Experimental evidence was obtained which indicates that this border observer (designated BO) moves upward relative to an external stationary observer (designated SO) at the same velocity as a moving observer (designated MO) located at the center of a bubble. In other words, evidence indicates that the PB-film border does not move relative to the rising bubbles. However, for the sake of greater generality in derivation, $v_{b,MO} \neq 0$ is allowed in the equations to follow, even though $v_{b,MO} = 0$ will actually be employed in final application.

OVERALL FLOW

The velocity profiles developed in the previous section are for an individual PB in some particular orientation. Those intermediate results will now be used to obtain an overall picture of the flow of liquid through a foam.

Consider a horizontal plane cutting through a vertical foam column of cross-sectional area A_{col}, exposing cross sectional areas totaling A_s in all PBs cut. Since the probable number of intercepted PBs oriented at θ is $P \sin\theta \cos\theta\, d\theta$, the net rate of volumetric flow upward relative to a stationary observer can be expressed by Equation (19) in terms of the local linear velocities upward through the cutting plane:

$$q_{col\ up,SO} = \int_{A_{PB}} \int_0^{\pi/2} v_{up,SO} P \sin\theta \cos\theta d\theta\, dA_s \qquad (19)$$

But $dA = \sin\theta\, dA_s$. Furthermore P is constant. Substitution in Equation (19) yields

$$q_{col\ up,SO} = P \int_0^{\pi/2} \int_{A_{PB}} v_{up,SO}\, dA \cos\theta d\theta \qquad (20)$$

Now consider $v_{s,SO}$ and $v_{b,MO}$ for a vertical PB. Then for a PB inclined at angle θ from the horizontal, the corresponding velocities are $v_{s,SO}\sin\theta$ and $v_{b,MO}\sin\theta$. Thus the component balance within such an inclined PB is

$$v_{up,SO} = v_{f,SO} - v_{s,SO}\sin^2\theta - v_{b,MO}\sin^2\theta \qquad (21)$$

as can be seen from Figure 7.*

In the above derivation it is implied that r_c is uniform for a horizontal cross section through the column, which is certainly reasonable. Were it otherwise, liquid would quickly flow from the thicker PBs to the thinner PBs by virtue of Equation (4) until all were of equal r_c.

Also implied is that the bulk foam rises through the column in plug flow. This is generally the case and is due in part to the inherent rigidity of the bulk foam. However physical obstacles or severely destructive foam breakage in the column can modify the usual configuration of plug flow.

Equations (22) to (27) define dimensionless groups where $v_{s,max,SO}$, $v_{s,SO}$, and $v_{b,MO}$ refer to a vertical PB. These three velocities thus serve as reference quantities independent of actual PB orientation:

$$Q_{col\ up,SO} = \frac{q_{col\ up,SO}}{P\, A_{PB}\, v_{s,max,SO}} \qquad (22)$$

* An important internal check of consistency is that the model predicts local material balance around any intersection of Plateau borders. It can be shown that this follows, regardless of orientation, from the symmetry of the four-way intersection and the proportionality of individual PB flow to $\sin\theta$.

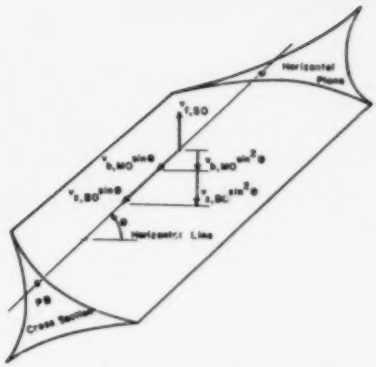

Fig. 7. Velocity components in a Plateau border.

$$dA^* = \frac{dA}{A_{PB}} \qquad (23)$$

$$V_{up,SO} = \frac{v_{up,SO}}{v_{s,max,SO}} \qquad (24)$$

$$V_{f,SO} = \frac{v_{f,SO}}{v_{s,max,SO}} \qquad (25)$$

$$V_{s,SO} = \frac{v_{s,SO}}{v_{s,max,SO}} \qquad (26)$$

$$V_{b,MO} = \frac{v_{b,MO}}{v_{s,max,SO}} \qquad (27)$$

Equations (22) to (27) are then substituted into Equations (20) and (21) which in turn are combined with each other. Analytical integration is then performed term by term to the extent feasible. This yields

$$Q_{col\ up,SO} = V_{f,SO} - \frac{V_{b,MO}}{3} + Q^*_{col\ up,SO} \qquad (28)$$

where

$$Q^*_{col\ up,SO} = -\int_0^{\pi/2} \int_{A^*_{PB}} V_{s,SO}\sin^2\theta\cos\theta d\theta dA^* \qquad (29)$$

Equation (30) is a useful alternative form of Equation (28):

$$Q_{col\ down,SO} = \frac{V_{b,MO}}{3} - V_{f,SO} + Q^*_{col\ down,SO} \qquad (30)$$

Equations (28) and (30) show that for $v_{b,MO} = 0$, the net upflow relative to the stationary observer equals the upflow as though the interstitial liquid were frozen, minus the actual downflow relative to the moving observer. Also, it is convenient to note that for $v_{b,MO} = 0$, subscripts BO and MO become equivalent to each other.

$Q^*_{col\ down,SO}$ is a function of M and T. This is shown in Figure 8. The function was obtained with the digital computer by numerically performing the double integration of Equation (29) for the various velocity profiles such as those of Figures 4, 5, and 6.

By extending this analysis further for $v_{b,MO} = 0$, $Q_{col\ up,SO}$ was separated into its upward moving portion $Q_{up,SO}$ and its downward moving portion $Q_{down,SO}$. This was carried out for various values of T. Figure 9 shows the numerically obtained results for $T = 0$. The dotted curve, which applies to hypothetical plug flow within each PB, was also derived analytically.

All of the foregoing analysis also applies to a stationary

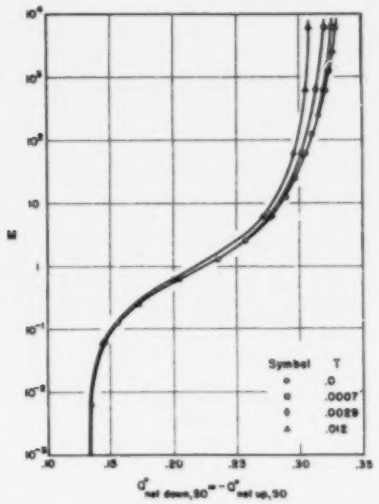

Fig. 8. Dimensionless relationship for flow through the foam as a whole.

foam; that is, where $v_{f,s0} = 0$, provided the rate of feed equals the rate of withdrawal from the bottom so as to maintain steady state.

In principle, the basic theory developed here should be extendible to foam draining at unsteady state, provided the rate of drainage is slow enough to allow a varying steady state velocity profile in a PB to be applied at unsteady state. A differential material balance over an incremental height of column would also be involved. However, the authors have not yet digressed along this particular avenue of investigation.

FOAM DENSITY AND EXIT

An interesting consequence of the model is that the foam density should be substantially uniform along the column between any inlet or outlet stream and the inlet or outlet stream immediately above or below [which implies $dr_s/dz = 0$ in Equation (18)]. Thus, in Figure 1 for example, $\mathcal{D}$ should be uniform from the feed inlet on down to the surface of the liquid pool.

That this should be so can be seen by considering the foam densities at any two different levels in the bottom section of the column. By simple material balance, $q_{net\ down,s0}$ at the lower level must equal that at the higher level. If $\mathcal{D}$ were greater at the lower level than at the higher level, A_{PB} would also have to be greater at the lower level since A_{col} is fixed and P would not change unless there were bubble coalescence. With a greater A_{PB}, the resistance to interstitial flow would be reduced. However, the driving force g_{eff} would decrease only slightly because generally the dominant term by far in Equation (18) is g_s, which here is just g. Therefore, $v_{s,max,s0}$ would clearly be greater. [This may also be seen from Equations (6), (14), and (16) when combined with Figure 3.] Then, by substituting in the definition for $Q_{net\ down,s0}$ [which is analogous to Equation (22)], $Q_{net\ down,s0}$ would be smaller. Also, by substitution in Equation (25), $V_{f,s0}$ would also be smaller since $v_{f,s0}$ would increase only slightly. Substituting these results in Equation (30) would make $Q^*_{net\ down,s0}$ decrease, since $V_{s,w0} = 0$. From Figure 8, this in turn would mean a smaller M, which by Equation (16) would yield a smaller r_s. By the geometry of the PB, a smaller r_s would mean a smaller A_{PB} and a smaller $\mathcal{D}$. However, this contradicts the original trial assumption of a higher $\mathcal{D}$ at this lower level, and so is absurd.

By a similar line of reasoning, an initial assumption of a smaller $\mathcal{D}$ at the lower level also results in an absurdity. Hence $\mathcal{D}$ at the lower level must equal that at the higher level. In other words, the foam density is uniform in the bottom section of the column.

The foam density should also be uniform in the top section of the column (above the feed point) but, of course, at a lower value than that in the bottom section. As before, this is predicated on the absence of coalescence.

In order to determine actual values for the foam density at the top of the column and the rate of overhead takeoff, it is first necessary to consider the manner of takeoff. Let the takeoff be through a smooth bend of uniform cross section equal to that of the column A_{col}. Equating $v_{f,s0}$ to the maximum downward velocity (relative to MO) in a PB averaged for the various orientations, one gets $v_{s,max,w0} = (3/2)\ v_{f,s0}$ at the top of the column. This situation will be termed here *normal exit*.

Actually, the particular choice of criteria for normal exit is not critical. In fact, in the earlier stages of the present study, the authors considered $v_{s,max,w0} = v_{f,s0}$. That choice yielded results which were not very different from those obtained with $v_{s,max,w0} = (3/2)\ v_{f,s0}$.

Normal exit requires that the bulk foam rise up the column substantially in plug flow (which should not be confused with plug flow within a PB). With a uniform A_{col} of more than several square centimeters this is essentially the case. However, obstructions in the column can cause sudden changes in $v_{f,s0}$, thus voiding the condition of normal exit.

The foam density at the top of the column can now be evaluated for normal exit by simultaneous trial and error solution of Figure 3 together with Equations (6), (8), (9), (12), (14), (16), (18), and (31):

$$v_{f,s0} = \frac{G}{A_{col}}\left(1 + \frac{V_L}{V_g}\right) \qquad (31)$$

Here, $v_{s,max}$ of Equation (14) is $v_{s,max,w0}$ which equals $(3/2)\ v_{f,s0}$ by virtue of normal exit. To simplify matters, Equation (18) usually can be approximated by $g_{eff} = g$. Also, $t = 0$ is usually satisfactory since the bubble films are very thin in the top section of the column.

After D has been found by Equation (32) as discussed later, W is obtained from Equation (1). By simple conservation of mass, $q_{net\ down,s0} = W$. Then the foam density in the lower section of the column, that is, below the feed point, can be evaluated by simultaneous trial and error solution of Figures 3 and 8 and Equations (6), (7), (8), (9), (12), (14), (16), (18), (25), (30), (31), and (22) with subscript net down replacing net up. With dp_{net}/dz primarily

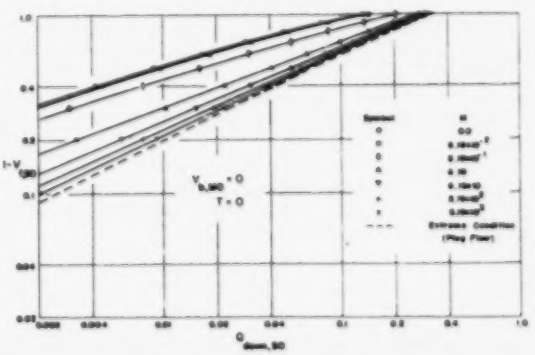

Fig. 9. Dimensionless relationship for exclusively downward flow through the foam as a whole.

due to the weight of the foam, Equation (18) can be well approximated by $g_{eff} = g(1 - \mathcal{D})$. Provision should be made for t.

Surface viscosity μ_s, for use in Equation (16) can be independently measured for the particular system by several methods (8, 21) including that employed in Part II of this paper. Alternatively, and perhaps more suitably for the present purpose, μ_s can be obtained by combining the theoretical relationships of the present part with a set of experimental results for the system in a properly operating foam column. This last method requires no concentration measurements and can be conveniently carried out with a rising or with a stationary foam. For the latter case, it might be added that since there is no overhead takeoff for a stationary foam, considerations relating to normal exit do not enter.

Approximate values of μ_s may also be found in standard references (8, 21) and other sources in the literature. For certain systems μ_s can vary markedly over narrow ranges of temperature.

Other physical properties can be obtained in the usual ways. For dilute solutions μ and ρ are often nearly those of the solvent.

The rate of collapsed overhead takeoff equals $q_{net\ up,so}$ at the top of the column. For normal exit, it is obtained with $v_{l,net,so} = (3/2)\ v_{l,so}$, and $v_{b,so} = 0$ by combining with Equations (7), (14), and (22) to give Equation (32):

$$D = 17.6(Q_{net\ up,so}H_{eff})\frac{A_{net}v^2_{l,so}}{h_{eff}d^2_m(1 + V_L/V_e)} \quad (32)$$

The quantity $Q_{net\ up,so}H_{eff}$ is a function of $\mu^2 v_{l,so}/\mu_s{}^2 h_{eff}$, which can be shown with $t = 0$ by simultaneous solution of Equations (6), (14), (16), (17), and (28) together with Figures 3 and 8. Figure 10 shows this function. Substitution in Equation (32) then gives D.

If t is known, $3tG/d_m$ can be added to D from Equation (32) to allow for the liquid carried out in the bubble faces. However, this is generally a very small contribution.

It should be noted that because of the velocity profiles within the PBs, $D/G \neq V_L/V_e$ at the top of the column. Rather, it can be shown from the foregoing that $1.25\ D/G < V_L/V_e < 2D/G$ at the top.

APPLICATION TO DESIGN

In predicting the performance of a foam fractionation column of the type described earlier and represented in Figure 1, Equation (32) is the key.

First, h_{eff} is obtained from Equation (12) with $g_{eff} = g$. Then, as a first trial, $\mathcal{D}$ in the upper part of the column can be assumed to be small. Thus V_L/V_e can be neglected, and $v_{l,so}$ is obtained from Equation (31). Substitution gives the quantity $\mu^2 v_{l,so}/\mu_s{}^2 h_{eff}$ from which the quantity $Q_{net\ up,so}H_{eff}$ is read from Figure 10. Substitution in Equation (32) yields D.

For fairly dry foam, D from the first trial can be accepted as is. For wetter foam, V_L/V_e can be calculated (by the trial and error procedure for $\mathcal{D}$ mentioned earlier) for use in a second trial. However, a quick approximation to the correction that would result is simply to multiply D by the quantity $(1 + 3D/G)$.

This correction factor is arrived at by taking V_L/V_e as approximately $1.6D/G$ and then by considering the various effects of V_L/V_e, namely on $v_{l,so}$ via Equation (31), on h_{eff} via Equation (18) with $\frac{dp_{net}}{\rho dz} = \frac{1.6Dg}{G}$, on the middle region of Figure 10, and finally on D itself via Equation (32). The correction is usually modest. Any contribution to dp_{net}/dz occasioned by frictional resistance to the bulk movement of the foam is neglected here. The small amount of liquid in the bubble faces is also neglected.

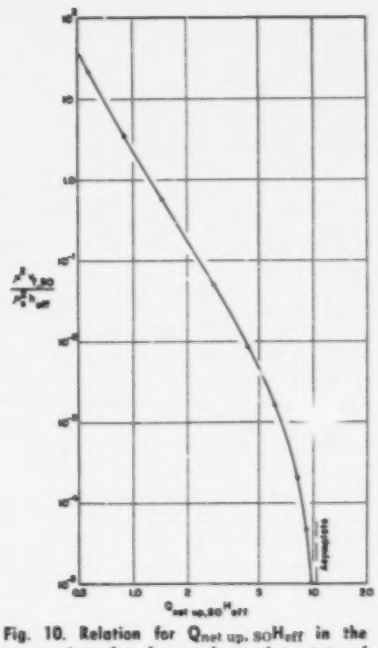

Fig. 10. Relation for $Q_{net\ up,so}H_{eff}$ in the top section of a foam column. Asymptote of 10.6 shown for $\mu_s = \infty$ or $v_{l,so} = 0$.

[The surface viscosity for use in Figure 10 can be obtained as described earlier. If a determination by flow through a stationary foam is selected, it is advisable to conduct the experiment before the foam grows too old. Otherwise, the larger bubbles in the foam will grow at the expense of the smaller bubbles because of the slight difference in pressure which causes gas to diffuse across the films. In some cases, appreciable changes in bubble size distribution can be observed in less than an hour. In such cases, the new distribution of bubble diameters must be employed.

For fairly rigid PB walls, as is often the case in foams of protein origin (8), precision in the determination of the high surface viscosity is not necessary. This is evident from Figure 10 wherein the curve approaches an asymptote. In fact, simply setting $\mu_s = \infty$ may be quite satisfactory in such cases. However, this simplification is not advisable for detergent foams because their PB walls are generally far from rigid (8).]

Corrected D is subtracted from F by Equation (1) to yield W.

With the feed point sufficiently far above the liquid pool so that C_L may be taken as equal to C_F, Equations (1) and (3) can be combined to give $C_W = C_F - \frac{6G\Gamma}{Wd_m}$. Substitution yields C_W. Then, substitution in Equation (2) yields C_D. Since the diameter is that for the bubbles as spheres in the liquid pool, strictly speaking the constant 6 should be replaced by 6.59 to account for their distortion to regular dodecahedra in the foam.

If column operation is altered so that the feed enters the liquid pool directly, C_L in Equation (3) should be replaced by C_W. Combination with Equation (1) yields $C_W = C_F - \frac{6G\Gamma}{Fd_m}$. The replacement of 6 by 6.59 should not apply to this last equation. The bubbles distort only after they have left the liquid pool. Thus the incremental

adsorption due to distortion is only gained at the expense of solute in interstitial liquid which is not replaced by any rinsing feed.

Prediction of performance is sensitive to bubble size. If the size is not uniform, the distribution must be known with some accuracy. Then d_{32} and d_m should be calculated from Equation (33) which is general for d_{ab}:

$$d_{ab}^{a-b} = \frac{\sum_i n_i d_i^a}{\sum_i n_i d_i^b} \tag{33}$$

Column height does not enter into the calculation of D. Indeed, except for insuring $C_L = C_F$ for side feeding, it is not involved at all. Thus, making the column still taller should not affect C_P. However, it must be remembered that the analysis is based on the absence of bubble coalescence in the column. Actually, increasing the height increases the residence time of the foam and so could promote coalescence. For the same reason, so could decreasing the gas rate. Coalescence would decrease D and increase C_L through internal reflux, thus increasing C_P. If such be the case it is recommended that d_{32} be taken at the top of the column. To estimate how d_{ab} is altered by moderate coalescence, it may be approximated from a known d_{ab} in the same section* of the column with the relationship $\frac{d_{ab,2}}{d_{ab,1}} = \left(\frac{\mathcal{D}_1}{\mathcal{D}_2}\right)^{1/6}$ if the value of $\mathcal{D}_1/\mathcal{D}_2$ is available from measurement or some other source.

The method can also be applied to calculate takeoff rates from columns with external reflux. For such columns, Equation (32) is applied to the section above the reflux inlet.

By material balance, the recyclic nature of external reflux does not allow equality between C_R and C_L at steady state conditions lest the already high C_R build up to an impossible value. Thus, with external reflux, increasing the column height can be of importance by allowing for increased contact between downcoming reflux and rising foam.

The extent of enrichment in a finite refluxing column depends in part on the mass transfer coefficient and the magnitudes of the counter-flowing streams. These latter can be estimated by means of the present model. Such calculations show substantial internal recycle within the column.

In a previous investigation (5) a relationship between exit concentrations was developed for a refluxing column which is long enough to allow the concentration in the downflowing interstitial liquid at some level in the column to approach the concentration of the upflowing interstitial liquid at that level, provided the feed point is in the liquid pool. Equation (34) is an equivalent form of that relationship:

$$C_P = C_F + \frac{6\Gamma}{D' d_m} \tag{34}$$

If the feed point is well above the liquid pool so that an effective stripping section is included in the column, Equation (34) can be modified to Equation (35):

$$C_P = C_F + \frac{6\Gamma}{D' d_m} \tag{35}$$

To allow for the small incremental adsorption associated with dodecahedral distortion, the constant 6 in Equation (34) may be replaced by the quantity $\left(6.59 - \frac{0.59}{R+1}\right)$. In Equation (35), the constant 6 should be replaced by just 6.59.

Since $D' = D/(R+1)$, Equation (34) or (35) can be combined with Equation (32) and appropriate overall balances to yield concentrations and flow rates for the exit streams from the column. The general method is thus readily extended to include long refluxing enriching columns and long combined columns.

* Meaning not separated by an inlet or outlet stream.

SUMMARY

A new model to describe the interstitial flow and drainage in a stationary or moving foam of noncoalescing bubbles was proposed and developed for steady state conditions. It involved solving the differential momentum conservation equation for flow through a representative capillary (or Plateau border) of curved triangular cross section with nonrigid boundaries characterized by a Newtonian surface viscosity. A finite difference approach was employed with a digital computer to obtain the velocity profiles. These, in turn, were combined by digital computation with a velocity component balance accounting for the random orientation of capillaries and the upward movement (if any) of the bulk foam.

Results were obtained in generalized dimensionless form so as to enable prediction of foam densities and flow rates for a wide range of conditions. When combined with material balances and considerations relating to surface adsorption, surfactant concentrations and rates of flow for the exit streams from a foam fractionation column can be estimated. A procedure for carrying out this estimation is outlined, and an extension to coalescing foams is suggested.

Results of the theory have been confirmed by experiment. Details of this confirmation are presented in Part II.

LITERATURE CITED

1. Adamson, A. W., "Physical Chemistry of Surfaces," Interscience, New York (1960).
2. Bikerman, J. J., "Foams: Theory and Industrial Applications," Reinhold, New York (1953).
3. Bird, R. B., W. E. Stewart, and E. N. Lightfoot, "Transport Phenomena," Wiley, New York (1960).
4. Brady, A. P., and S. Ross, *J. Am. Chem. Soc.*, **66**, 1348 (1944).
5. Brunner, C. A., and R. Lemlich, *Ind. Eng. Chem. Fundamentals*, **2**, 297 (1963).
6. *Chem. Eng.*, **68**, No. 7, p. 100 (1961).
7. Corkill, J. M., J. F. Goodman, C. P. Ogden, and J. R. Tate, *Proc. Roy. Soc. (London)*, **Ser. A273**, 84 (1963).
8. Davies, J. T., and E. K. Rideal, "Interfacial Phenomena," Academic Press, New York (1961).
9. Gibbs, J. W., "Collected Works," Vol. 1, Longmans Green, New York (1928).
10. Haas, P. A., and H. F. Johnson, "A Model and Experimental Results for Drainage of Solution between Foam Bubbles," presented at Am. Chem. Soc. national meeting, Chicago, Illinois (Aug. 30 to Sept. 4, 1964).
11. Harper, D. O., and R. Lemlich, *Ind. Eng. Chem., Process Design and Devel. Quarterly*, **4**, 13 (1965).
12. Hildebrand, F. B., "Introduction to Numerical Analysis," McGraw-Hill, New York (1956).
13. Husmann, W., *Textil-Rundschau*, **17**, 88 (1962).
14. Jacobi, W. M., K. E. Woodcock, and C. S. Grove, Jr., *Ind. Eng. Chem.*, **48**, 2046 (1956).
15. Klein, S. A., and P. H. McGauhey, *Journal W.P.C.F.*, **35**, 100 (1963).
16. Lemlich, R., and E. Lavi, *Science*, **134**, No. 3473, p. 191 (1961).
17. Leonard, R. A., Ph.D. dissertation, University of Cincinnati, Cincinnati, Ohio (June, 1964).
18. ———, and R. Lemlich, *Chem. Eng. Sci.*, to be published.
19. Manegold, E., "Schaum," Strassenbau, Chemie und Technik Verlagsgesellschaft m.b.H., Heidelberg (1953).

20. Miles, G. D., L. Shedlovsky, and J. Ross, *J. Phys. Chem.*, 49, 93 (1945).
21. Mysels, K. J., K. Shinoda, and S. Frankel, "Soap Films, Studies of their Thinning and a Bibliography," Pergamon Press, New York (1959).
22. Osipow, L. I., "Surface Chemistry, Theory and Industrial Applications," ACS Monograph Series 153, Reinhold, New York (1962).
23. Ross, S., *J. Phys. Chem.*, 47, 266 (1943).
24. Rubin, E., and E. L. Gaden, Jr., "New Chemical Engineering Separation Techniques," Chap. 5, H. M. Schoen, ed., Interscience, New York (1962).
25. Schnepf, R. W., and E. L. Gaden, Jr., *J. Biochem. Microbiol. Tech. Eng.*, 1, 1 (1959).
26. ———, E. Y. Miroczník, and E. Schonfeld, *Chem. Eng. Progr.*, 55, No. 5, p. 42 (1959).

Manuscript received March 23, 1964; revision received August 14, 1964; paper accepted September 9, 1964.

Part II. Experimental Verification and Observations

Experimental results obtained over a wide range of variables from three different foam fractionation columns support the theory developed in Part I.

LITERATURE CITED

1. Bikerman, J. J., "Foams: Theory and Industrial Applications," Reinhold, New York (1953).
2. Crook, E. H., D. B. Fordyce, and G. F. Trebbi, *J. Phys. Chem.*, 67, 1987 (1963).
3. Fanlo, S., Ph.D. dissertation, University of Cincinnati, Cincinnati, Ohio, in preparation.
4. Greenwald, H. L., E. B. Kice, M. Kenly, and J. Kelly, *Anal. Chem.*, 33, 465 (1961).
5. Lauwers, A., P. Joos, and R. Ruyssen, "Third International Congress on Detergency, Vol. 3, Sec. C, p. 195, Cologne (1960).
6. Leonard, R. A., Ph.D. dissertation, University of Cincinnati, Cincinnati, Ohio (June, 1964).
7. Mysels, K. J., K. Shinoda, and S. Frankel, "Soap Films, Studies of their Thinning and a Bibliography," Pergamon Press, New York (1959).

Manuscript received March 23, 1964; revision received August 14, 1964; paper accepted September 9, 1964.

In Part I a theory was developed for interstitial flow in foam which could be applied to foam fractionation. This paper presents the results of experimental tests of this theory.

EXPERIMENTAL

A foam fractionation column of 4.1-cm. I.D. was constructed of glass as shown in Figure 1. Thoroughly humidified nitrogen was bubbled up through the liquid pool at the bottom, forming foam which rose up the column and passed out through the horiontal line of 0.8-cm. I.D. at the top. The liquid level of the pool at the bottom of the column was maintained approximately 80 cm. below the overhead foam line. The feed point and pressure probe were adjustable up and down the column. Operation was at 25° ± 1°C. in a temperature-controlled room. Further details of experiments and results have been placed on file (*6*).

A bubbler with a single orifice was employed in order to obtain a uniform bubble size for a given run. The frequency at which bubbles were formed was measured with a stroboscopic light. The bubble diameter was then calculated by $d_m = \sqrt[3]{6G/\pi N}$. The feed was a 5×10^{-4} molar aqueous solution of the surfactant Triton X-100, which can be considered to have the formula C_8H_{17}—⟨⟩—$(OCH_2CH_2)_{9.7}$—OH.

After a foam with bubbles of uniform size and known diameter had been formed, the gas flow to the bubbler was usually stopped. The liquid feed rate through the foam was continued for a while to achieve steady state conditions and to allow the flow rate to be checked. Then the feed line was closed and the bottom exit was blocked so that the volume of interstitial liquid in the foam could be measured when the foam collapsed. During these latter operations, the faces of the foam bubbles were observed in order to obtain a measure of their thickness by their progressive color changes with a technique (*1, 7*) based on the diffraction of incident light.

Two runs were made at continuous gas flow conditions. These required a much longer time to reach steady state and still longer to collect enough overhead foam for a measurement of collapsed volume. Furthermore, it was difficult to maintain the relatively dry foam in the necking section at the top of the column. The strain of the tenfold reduction in cross section would often suddenly collapse all the foam in the entire top section of the column, thus invalidating the run. Accordingly, most of the runs were not of this type involving continuous gas flow, since much of the information that could be obtained from this column could be gained just as well and more quickly by simply letting liquid flow down through stationary foam, that is with $v_{f,so} = 0$.

Surface tension was measured with a ring tensiometer yielding values close to those obtained by others (*2, 4*). Viscosity was measured with an Ostwald viscosimeter, yielding values close to those of pure water. Γ determined from surface tension via Gibbs' equation generally compared favorably with that determined from Equations* (2) and (3) from experiments with the foam column. Both methods yielded Γ of about 2.8×10^{-10} g. moles/sq.cm., except for very dry foams in which a micelle double film (*5*) may have formed. Solute concentrations were measured by ultraviolet spectrophotometry.

RESULTS

For each run, the experimental values for V_L/V_a, t, and $d_m = d_n = d_w$ were substituted in Equation (8) to give A_{rs}. This was for the section of column from the feed point down to the surface of the liquid pool. Substitution in Equation (6) gave r_s. T followed from Equation (17).

Measurements with the pressure probe showed that the entire weight of foam was transmitted as hydrostatic head. Observation of face colors showed no variation of t with height, which implies $dr_s/dz = 0$ and also a uniform foam density. This uniformity in $\mathcal{D}$ accords with the prediction

* All equation numbers refer to Part I.

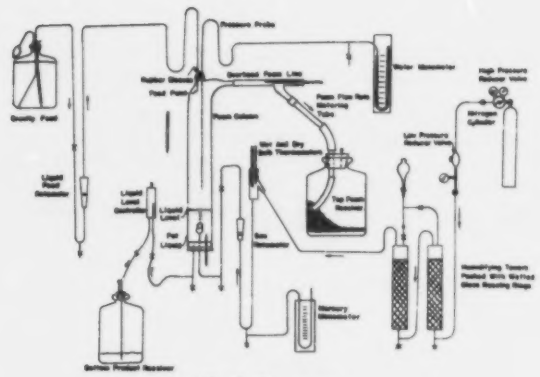

Fig. 1. Apparatus.

of theory in Part I.

Substitution in Equation (18) gave g_{eff}. Then $h_{eff} = \rho g_{eff}/\mu$ where ρ and μ were taken as those for pure water. Velocity $v_{f,so}$ was calculated from Equation (31). As pointed out above, it was zero for most runs. P was evaluated from Equation (7). In view of steady state operation, $W = q_{sat\ down,so} = -q_{sat\ up,so}$. Then μ_s was evaluated by simultaneous trial and error solution with Equations (14) (with $v_{s,max,so}$ replacing $v_{s,max}$), (16), (22), and (30), and Figures 3 and 8, with $v_{b,so} = 0$. Normal exit criteria were not involved here. For all the runs, the values of μ_s thus obtained ranged from 0.24×10^{-4} to 2.24×10^{-4} dyne sec./cm., with a standard deviation of 0.63×10^{-4} dyne sec./cm. The mean value of μ_s was 1.24×10^{-4} dyne sec./cm., with a 95% confidence interval of $\pm\ 0.40 \times 10^{-4}$ dyne sec./cm. by statistical t test.

At the conclusion of a run, while the foam in the column was allowed to drain preparatory to measurement of V_L/V_o, close inspection of bubbles through a magnifying glass revealed bits of black film forming at the bottom of a face and rising upward in the face. These bits appeared as little circles, each trailed by a thin wavey black tail as illustrated in Figure 2. These circles are local areas of extremely small film thickness and appear black by virtue of diffractive cancellation of light. Being thinner than the surrounding film they float up in the face under the influence of gravity.

A method has been proposed (7) whereby these black circles may be used in an independent manner to determine an approximate value for μ_s. Accordingly, for each of sixteen observations, an estimate was made of the film thickness, the inclination of the face, the diameter of the black circle, and the distance the circle moved within the face in a timed interval. These rough measurements were then substituted in the equation given below, which is essentially the surface analogue of Lamb's classical solution

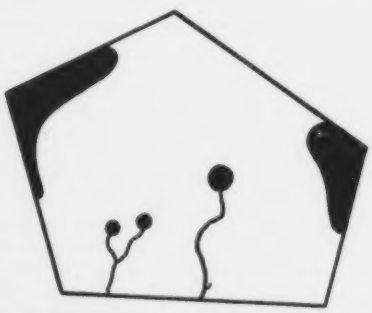

Fig. 2. Typical pattern of black in white film, showing the rising black circles.

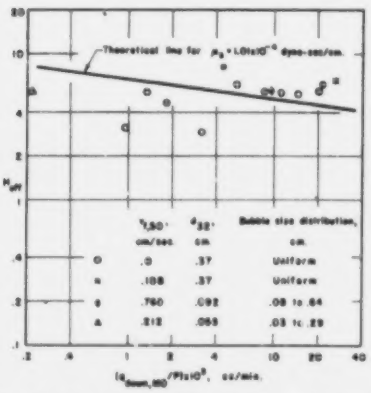

Fig. 3. Experimental results for flow through foam.

for a buoyant, infinitely long, horizontal cylinder rising at terminal velocity in a homogeneous viscous fluid.

$$\mu_s = \frac{-r_c^3 \rho g (t - t_b)\cos\varphi}{8u}\left[0.0772 + \ln\frac{u\, r_c\, \rho t}{8\,\mu_s}\right] - \frac{\mu t}{2}$$

The last term was negligible. Solving by trial yielded values of μ_s ranging from 0.38×10^{-4} to 1.55×10^{-4} dyne sec./cm. with a standard deviation of 0.47×10^{-4} dyne sec./cm. The mean value of μ_s was 1.01×10^{-4} dyne sec./cm., with a 95% confidence interval of $\pm\ 0.25 \times 10^{-4}$ dyne sec./cm.

When one considers the various experimental uncertainties, μ_s of 1.01×10^{-4} dyne sec./cm. determined from the black circles agrees fairly well with μ_s of 1.24×10^{-4} dyne sec./cm. determined from interstitial flow through foam. This supports the theory developed in Part I. It should be added that altering the theoretical model by assuming $v_{b,so} \neq 0$ yielded no better agreement.

Figure 3 shows experimental results plotted as H_{eff} vs. $q_{down,so}/P$, which is a proportional measure of the flow rate through a Plateau border. For stationary foam, $v_{f,so} = 0$, and so $q_{down,so} = q_{sat\ down,so} = W$. For moving foam, $q_{down,so} = W + PA_{PB}v_{f,so}$. Also shown are the results for two additional runs with a multiorificed bubbler that produced a very nonuniform distribution of bubble sizes. For these two runs the distribution was determined by count and measurement of individual bubbles in the narrow part of the neck at the top of the column. This was the original purpose of constructing the narrow takeoff.

For comparison, Figure 3 also shows a curve for H_{eff} vs. $q_{down,so}/P$ determined from the theory of Part I by use of the value of μ_s derived by the independent black circle method. The theoretical curve is seen to pass through the general region of the data. In view of the range of variables and the experimental uncertainties, this is deemed to be good agreement.

ADDITIONAL COMPARISONS

Further confirmation for the theory was obtained from the experimental values for the overhead flow D in the runs with $v_{f,so} \neq 0$. This was bolstered with additional runs made very early in the investigation with a nonuniform bubbler in another column designed to accommodate removable plates. (These plates proved to be of no particular advantage.)

Runs for which the feed point was above the exit plane were discarded. Also discarded were runs in which large

wall-to-wall slugs of gas were present, indicating severe breakage of foam. Finally, only runs for which the bubble size distribution was measured along the outlet tube atop the column were used. Measurement of bubble size at the side of a column can sometimes be misleading, since the larger bubbles tend toward the center line and thus are hidden from view by the smaller bubbles at the wall. Furthermore, as pointed out in Part I, taking the bubble sizes at the top minimizes the effect of coalescence on the theory.

A total of eight runs met these criteria. These covered a fairly wide range of experimental variables, namely D from 0.062 to 0.305 cc./sec., $v_{f,s0}$ from 0.22 to 0.78 cm./sec., and d_n from 0.05 to 0.11 cm. For each run, experimental D was compared with theoretical D from Equation (32) based on the independently determined value of μ, $= 1.01 \times 10^{-4}$ dyne sec./cm. Over the eight runs, the ratio of theoretical D to experimental D ranged from 0.86 to 1.95, with a standard deviation of 0.36. The mean ratio was 1.38 ± 0.30 at the 95% confidence level. This is considered reasonably good agreement. However, the modest positive difference over unity is statistically significant. It could be due to the effect of the sharp reduction in cross section experienced by the foam as it enters the outlet tube. It could also be indicative of some experimental bias in determining the bubble size distribution from the nonuniform bubbler employed for these runs. Error at the small diameter end of the distribution curve is especially critical.

Profiting from experience with the columns described above, a different but related investigation was begun. In this new study (3), a foam column was constructed with an overhead takeoff which was not necked. Bubble size distributions were determined visually or photographically at the surface of the liquid pool. Then, as described in Part I, these were corrected for coalescence within the column up to the exit by means of electrical conductivity measurements of foam density.

Some preliminary data from this new study are available. Column diameter is 4.6 cm., which is slightly larger than heretofore. Calibration runs with feed entering near the top showed a uniform foam density, which conforms with the theory. Five usable runs are available with feed entering the liquid pool. D ranged from 0.0014 to 0.0306 cc./sec., $v_{f,s0}$ from 0.082 to 0.195 cc./sec., and d_n from 0.11 to 0.24 cm. Again utilizing the independent μ, of 1.01

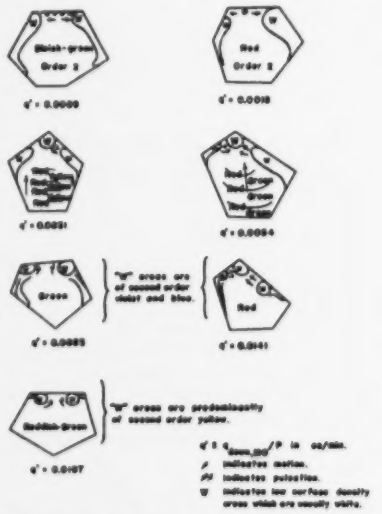
Red
Order 2
Green
Red
Green
Red
Green
Red

The average film thickness increased with the average flow rate through a Plateau border. This is shown in Figure 5, for which C_L was about 5×10^{-7} g.-moles/cc. The dimensionless thickness T increased approximately linearly from 1.5×10^{-6} to 6×10^{-6} over the same range of experimental $q_{down,MO}/P$.

SUMMARY OF CONCLUSIONS

Observations and flow measurements at steady state were taken in a specially constructed foam column employing stationary foams and moving foams. When combined with surface viscosity measured by an independent method, the experimental results were in substantial agreement with those predicted by the theory developed in Part I. Additional confirmation of the theory was obtained with experimental results from two other columns.

ACKNOWLEDGMENT

The work in Parts I and II was supported directly by U.S. Public Health Research Grant WP-161. Indirect support was derived from the National Science Foundation through grant G-19281 at the University of Cincinnati Computer Center and through a Cooperative Fellowship.

NOTATION

dA = differential area situated in A_{PB}, sq.cm.
dA^* = dA/A_{PB}
A^* = dimensionless A_{PB}; that is, unity
a = PB dimension as shown in Figure 2*c*, cm.
A_{col} = horizontal cross-sectional area of a foam column, sq.cm.
A_h = that part of the horizontal cross-sectional area of a column which cuts through the PBs, sq.cm.
A_{PB} = perpendicular cross-sectional area of a PB, sq.cm.
C = concentration of the surfactant per unit volume of solution, g.-moles/cc.
D = volumetric flow rate of the collapsed overhead foam; that is, of just the liquid content, cc./sec.
D' = volumetric flow rate of the collapsed net overhead product withdrawn when reflux is employed, cc./sec.
$\mathcal{D}$ = volumetric foam density
d_{ab} = average bubble diameter, cm.
d_i = particular bubble diameter, cm.
d_m = bubble diameter averaged by volume and number of bubbles, cm.
d_n = bubble diameter averaged by volume and diameter, cm.
d_s = bubble diameter averaged by volume and area, cm.
E = length of PB, cm.
e = integer
F = volumetric feed rate, cc./sec.
G = volumetric flow rate of gas, cc./sec.
g = gravitational acceleration, cm./sec.^{2}
g_{eff} = effective gravitational acceleration, cm./sec.^{2}
H_{eff} = dimensionless hydrodynamic driving force, $h_{eff}A_{PB}/v_{s,max,BO}$
h_{eff} = $\rho g_{eff}/\mu$, cm.$^{-3}$ sec.$^{-1}$
i = index
k = integer
M = dimensionless viscosity ratio, $\mu r_o/\mu_s$
N = number of bubbles formed per unit time, sec.$^{-1}$
n_i = number of bubbles with diameter d_i
P = packing factor, the total length of PBs within a unit height of foam column
p_{in} = pressure inside the PB, dynes/sq. cm.
p_{out} = pressure outside the PB, dynes/sq. cm.
Q = dimensionless volumetric flow rate, $q/(PA_{PB}v_{s,max,BO})$
q = volumetric flow rate, cc./sec. or cc./min.
q' = $q_{down,MO}/P$, cc./min.
R = reflux ratio
r = radial coordinate, cm.
r_c = radius of a black circle, cm.
r_o = radius of curvature of PB-gas interface, cm.
T = dimensionless cross sectional aspect ratio for a PB, t/r_o
t = film (face) thickness, cm. or microns
t_b = film thickness of a black circle, cm. or microns
u = velocity of a black circle moving within a face, cm./sec.
V_{liq} = volume of liquid in all the PBs confined in the incremental height H, cc.
V = dimensionless velocity, $v/v_{s,max,BO}$
v = velocity cm./sec.
V_g = volume of gas in a $(V_L + V_g)$ volume of foam, cc.
V_L = volume of liquid in a $(V_L + V_g)$ volume of foam, cc.
W = volumetric bottom product rate, cc./sec.
z = axial coordinate along the PB axis which may be particularized as being vertically downward, cm.

Greek Letters

Γ = surface excess, g.-mole/sq.cm.
γ = surface tension, dynes/cm.
ϵ = void (gas) fraction in the foam
θ = angle which the PB makes with the horizontal
μ = viscosity, dyne sec./sq.cm.
μ_s = surface viscosity, dyne sec./cm.
ρ = liquid density, g./cc.
τ = time, sec.
φ = angle of inclination between the bubble face and the vertical

Subscripts

b = in an axial (z) direction at the border between the PB and the bubble film (such as at point A of Figure 2)
BO = with respect to an observer located at the border between the PB and the bubble film (such as at point A of Figure 2)
D = collapsed overhead foam
down = downward
F = feed
f = of the foam, taken in a vertically upward direction when applied to the foam velocity
L = interstitial liquid free of Γ in the overhead foam
max = maximum, that is at point 0 of Figure 2, which in some contexts is particularized for a vertical PB
MO = with respect to an observer moving with the same vertical velocity as the aggregate of foam bubbles
net = net
r = in a radial direction
R = reflux
SO = with respect to a stationary observer
up = upward
W = bottom liquid product
z = in an axial direction which may be particularized as being vertically downward
θ = in an angular direction
1 = at some level in the column
2 = at another level in the same continuous section of the column

Superscript

o = taken at $V_{f,BO} = 0$ and $V_{b,MO} = 0$

Chemical Engineering Science, 1965, Vol. 20, pp. 790–791. Pergamon Press Ltd., Oxford. Printed in Great Britain

Laminar longitudinal flow between close-packed cylinders

(*Received* 17 *August* 1964)

RECENTLY, GUNN and DARLING [1] presented numerical solutions and experimental results for steady longitudinal flow through several interesting cross-sections, together with a literature survey dealing with several others. However, their paper does not include flow between close-packed congruent circular cylinders; that is, between (along) mutually tangential parallel circular cylinders on equilateral triangular pitch. Accordingly, the present writers offer here a solution for steady laminar longitudinal flow through this cross section.

The present report is an outgrowth of a larger investigation into interstitial flow through foam [3]. Such flow occurs through capillaries (Plateau borders). In one limiting case, the walls of such a capillary are rigid and in the shape of tangential circular arcs as shown by the heavy solid curves of Fig. 1. This cross-section is obviously identical with that for the free space between tangential parallel congruent circular cylinders. The dotted circles superimposed in Fig. 1 illustrate this.

In cylindrical co-ordinates, the equation for steady laminar longitudinal flow of an incompressible fluid is

$$\frac{\partial^2 u}{\partial r^2} + \frac{1}{r}\frac{\partial u}{\partial r} + \frac{1}{r^2}\frac{\partial^2 u}{\partial \theta^2} - \frac{1}{\mu}\frac{dp}{dz} = 0 \qquad (1)$$

Equation (1) was conveniently applied with point 0 as origin. The cross-section involves six-fold symmetry so that solution was required only for the region *RMT*. Boundary conditions were zero velocity at $r = r_0$, angular symmetry across *RM*, and mirror symmetry across *MT*.

Equation (1) was solved by converting it into its analogous difference equation for a grid of fifty-three nodal points. For a typical interior point at r and θ the difference equation yielded

$$\left(\frac{r\Delta\theta}{\Delta r} + \frac{\Delta\theta}{2}\right)u(r + \Delta r, \theta) + \left(\frac{\Delta r}{r\Delta\theta} - \frac{\Delta\theta}{2}\right)u(r - \Delta r, \theta) + \frac{\Delta r}{r\Delta\theta}u(r, \theta + \Delta\theta) + \frac{\Delta r}{r\Delta\theta}u(r, \theta - \Delta\theta) - 2\left(\frac{r\Delta\theta}{\Delta r} + \frac{\Delta r}{r\Delta\theta}\right)u(r, \theta) - \frac{r\Delta r\Delta\theta}{\mu}\frac{dp}{dz} = 0 \qquad (2)$$

The set of simultaneous equations so developed was solved by CROUT'S matrix reduction [2] on an I.B.M. 1620 digital computer.

Integrating the resulting velocity profile over the cross-section yielded

$$u_m = 2{\cdot}49\bar{u} \qquad (3)$$

The equation for viscous drag is

$$-\frac{dp}{dz} = \frac{2k\mu\bar{u}}{D_H^2} \qquad (4)$$

For the present cross-section, $D_H = 0{\cdot}205r_0$ and $k = 6{\cdot}43$. This can be compared with the familiar flow through a circular cross-section for which $u_m = 2\bar{u}$, $D_H = D$ and $k = 16$. Results agree very well with those of SPARROW and LOEFFLER [4].

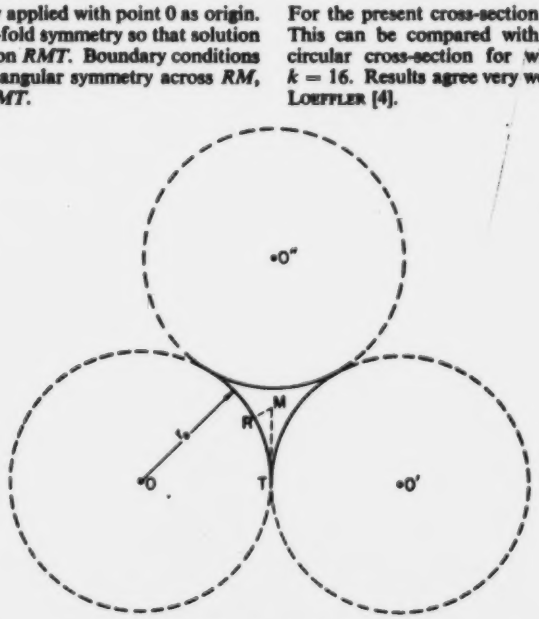

FIG. 1. Close-packed cylinders.

* Present address: E. I. du Pont de Nemours & Co., Engineering Research Division, Wilmington, Delaware, U.S.A.

The aforementioned results apply only to laminar flow. However, GUNN and DARLING have proposed a general method for estimating friction in turbulent flow from friction in laminar flow.

Acknowledgement—This work was supported directly by U.S. Public Health Research Grant WP-161. Indirect support was derived from the National Science Foundation through grant G-19281 at the University of Cincinnati Computing Center and through a Co-operative Fellowship.

R. A. LEONARD* and R. LEMLICH

Department of Chemical Engineering,
University of Cincinnati
Cincinnati, Ohio 45221

NOTATION

D	Diameter of circle	cm
D_H	Hydraulic diameter equal to four times the cross-sectional area divided by the wetted perimeter	cm
k	Constant	dimensionless
r	Radius	cm
r_0	Radius of cylinder	cm
p	Pressure	dyn/cm²
u	Velocity of flow	cm/sec
u_m	Maximum velocity of flow	cm/sec
$\bar{u}$	Average velocity of flow	cm/sec
z	Axial distance	cm
θ	Angle	radians
μ	Dynamic viscosity	dyn sec/cm²

REFERENCES

[1] GUNN D. J. and DARLING C. W. W., *Trans. Instn. Chem. Engrs* 1963 **41** 163.
[2] HILDEBRAND F. B., *Introduction to Numerical Analysis*. McGraw-Hill, New York 1956.
[3] LEONARD R. A. and LEMLICH R., *J. Amer. Inst. Chem. Engrs*. 1965 **11** 18.
[4] SPARROW E. M. and LOEFFLER A. L. JR. *J. Amer. Inst. Chem. Engrs*. 1959 **5** 325.

(*Reprinted from Nature, Vol. 207, No. 4993, pp. 145-146, July 10, 1965*)

SEPARATION OF LIQUID MIXTURES BY NON-FOAMING BUBBLE FRACTIONATION

By DENNIS C. DORMAN and PROF. ROBERT LEMLICH

Department of Chemical Engineering, University of Cincinnati, Cincinnati, Ohio

OVER the past few years there has been increased interest in the technique of partially separating (concentrating) the components of a liquid mixture by means of foam fractionation. Studies reported include those of our own group[1-4], as well as those of a number of other investigators[5] including one investigation which appeared recently in *Nature*[6].

Foam fractionation is based on the preferential adsorption of a solute at the interface of bubbles which are usually formed by deliberately bubbling a gas through a liquid mixture. These bubbles rise, forming a foam which carries the solute off overhead, thus effecting a partial separation of components. Unfortunately, by its very nature, use of the technique is limited to systems which will in fact foam. Accordingly, the present investigation was initiated to examine the feasibility of using a 'foamless foam column'; that is, just a vertically elongated pool of liquid. So far as we are aware, this has been a virtually neglected area of study.

The simple device used is shown in Fig. 1*a*. It is called a 'bubble column' in contradistinction to a foam column. In the work recorded here it was a vertical glass tube filled to a convenient height with a very dilute aqueous solution of a surface-active agent, namely, technical monobutyl diphenyl sodium monosulphonate. Nitrogen gas (which was first thoroughly humidified to eliminate subsequent evaporation) was bubbled up through the liquid in the column. The objective was to see whether a significant concentration gradient would occur in the column despite the fact the solution was too dilute to foam.

After bubbling for several hours at room temperature, samples were withdrawn from the top and bottom of the column and analysed for solute spectrophotometrically by the standard methylene blue test[7]. A number of runs were conducted. For initial charge concentrations of several parts per million, the concentration at the top was as much as quadruple that at the bottom. Such marked separation shows that, even at concentrations

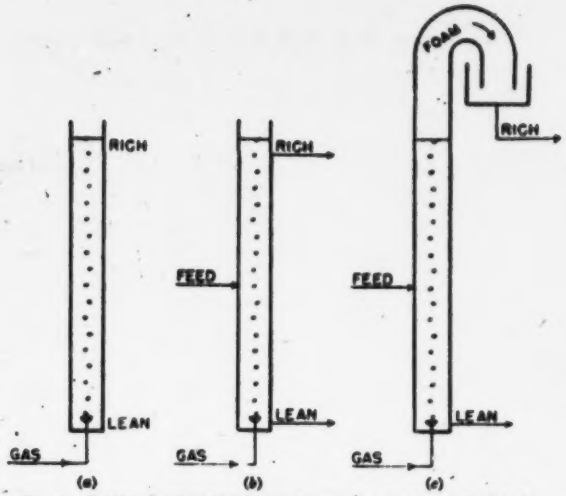

Fig. 1. Bubble fractionation apparatus (not to scale). *a*, Batchwise operation as used here; *b*, projected flow operation; *c*, projected application to low-threshold foam fractionation

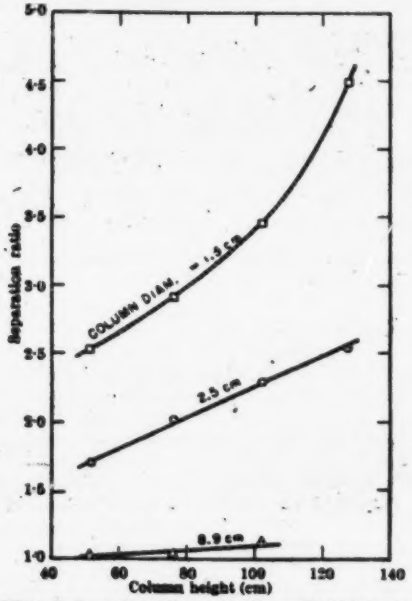

Fig. 2. Effect of column dimensions on the degree of bubble fractionation for a charge concentration of 3·1 parts per million

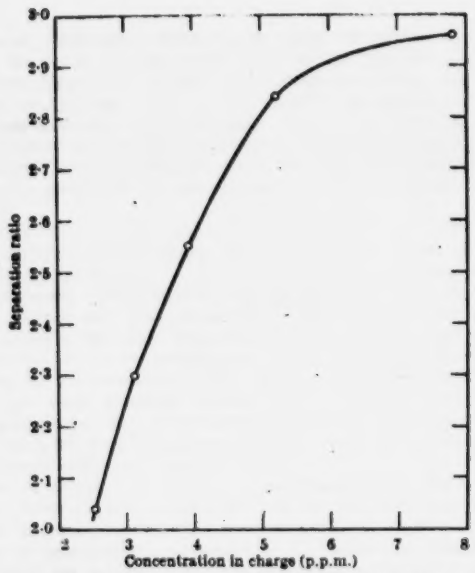

Fig. 3. Effect of charge concentration on the degree of bubble fractionation in a column of 2·5 cm diameter and 102 cm height

below the foaming threshold, the rising bubbles were quite effective in adsorbing solute at their surfaces and carrying it to the top of the column. (Bubble fractionation is based on surface adsorption of non-volatile solute and should not be confused with the familiar but quite different operation of desorption which involves diffusion of volatile solute into the bubble interior.) This transport establishes the concentration gradient within the column.

Of course, the operation has its internal limitations. The rising bubbles drag lean liquid from the bottom up to the top. Rich liquid from the top then flows down to the bottom as replacement. The mixing action of this circulation limits the separation attainable.

With bubble sizes in the narrow range of 0·36–0·38 cm diameter, varying the frequency from 120 to 250 bubbles per min was of comparatively little effect. This accords with the aforementioned limitation. Increasing the bubble frequency increases the undesirable mixing as well as the desirable adsorbing surface.

Fig. 2 and Fig. 3 show the effects of several independent variables on the separation ratio (which is defined as the ratio of the concentration at the top of the column to that at the bottom of the column). The degree of separation increased with the height of the liquid column and with the charge concentration, but decreased with the column diameter. This last would seem to result from a wall effect which is diminished at larger diameters, thus allowing the aforementioned undesirable circulation to proceed with less hindrance.

The experiments performed here were in batch. However, with sufficient hold-up (liquid residence time) it should be possible to operate continuously as shown in Fig. 1b. Finally, for a solution the concentration of which is only slightly below the foaming threshold, it should be possible to enrich the top of the liquid sufficiently by bubble fractionation so that foam fractionation could be used above it. This is illustrated in Fig. 1c.

This work was supported in part by U.S. Public Health Service research grant *WP*–161.

[1] Lemlich, R., and Lavi, E., *Science*, **134**, No. 3473, 191 (1961).
[2] Brunner, C. A., and Lemlich, R., *Indust. Eng. Chem. Fundamentals Quart.* **2**, 297 (1963).
[3] Harper, D. O., and Lemlich, R., *Indust. Eng. Chem. Process Design and Development Quart.*, **4**, 13 (1965).
[4] Leonard, R. A., and Lemlich, R., *Amer. Inst. Chem. Engrs. J.*, **11**, 18, 25 (1965).
[5] For some recent listings, see Grieves, R. B., and Wood, R. K., *Amer. Inst. Chem. Eng. J.*, **10**, 456 (1964).
[6] Grieves, R. B., and Wood, R. K., *Nature*, **200**, 332 (1963).
[7] *Standard Methods*, 246 (American Public Health Association, New York, 1960).

Printed in Great Britain by Fisher, Knight & Co., Ltd., St. Albans.

Reprinted from I&EC PROCESS DESIGN AND DEVELOPMENT, Vol. 4, Page 13, January 1965
Copyright 1964 by the American Chemical Society and reprinted by permission of the copyright owner

BUBBLE AND FOAM FRACTIONATION COMBINED

DEAN O. HARPER AND ROBERT LEMLICH

Chemical Engineering Department, University of Cincinnati, Cincinnati 21, Ohio

Experiments were carried out to examine the desirability of operating a combined column consisting of a refluxing foam fractionating section situated immediately above a bubble fractionating section. The range of column operability and the over-all effects of several variables were studied.

In recent years there has been something of a reawakening of interest in the separation of mixtures by foam fractionation. What was originally a laboratory curiosity is now commanding more serious attention. An extensive review of the literature has recently appeared (*5*).

Foam fractionation involves the adsorption of solute at the surfaces of bubbles formed by sparging. These bubbles form a column of foam above the main liquid interface. Natural drainage and deliberate reflux (*2, 3*) improve the over-all separation.

A foam fractionation column can be operated as an enricher, a stripper, or a combined column. However, experiments along these lines to date have been chiefly directed at the separation which takes place in the foam column per se. By comparison, the separation which takes place in the pool of liquid at the bottom of the column seems to have been largely taken for granted.

Accordingly, in the present investigation the height of the liquid pool was deliberately increased to become what is termed here a "bubble column" (in contradistinction to a foam column). Of course, a bubble column can be used alone as a stripper, especially at low concentrations. (This was confirmed by preliminary experiment.) However, in the present investigation it is combined with a foam column. With the bubble column more suited to the lower concentration at the bottom, and the foam column more suited to the higher concentration at the top, the combination should bring out the best features of each.

Experimental

The fractionating column was of glass, 4.8 cm. in inside diameter and 174 cm. tall. For each run a 2.2×10^{-4} M aqueous solution of the commercial surfactant Triton X-100 [*tert*-C_8H_{17}-ϕ-$(OCH_2CH_2)_{9.7}OH$] was fed in at 32 ml. per minute to one of three feed locations. Thoroughly humidified nitrogen was introduced through a coarse sintered-glass bubbler near the bottom of the column. Foam was withdrawn from the top and collapsed in a rotary foam breaker, and a portion thereof (ranging from none to all) was returned as reflux to a point near the top of the column. Stripped liquid was withdrawn from the bottom. The interface between the liquid section (which comprises the bubble column) and the foam section (which comprises the foam column) was maintained at a height of 110 cm., thus fixing the length of the two sections. A schematic diagram of the apparatus is shown in Figure 1.

Factorial experiments were carried out to examine the effects of varying the gas flow rate, the reflux ratio, and the feed location. The three positions for this last variable were at heights of 53, 105, and 126 cm. The middle height was deliberately selected close to but not exactly at the dividing interface between the two column sections, in order to avoid any complications which might arise from slight shifts in the precise level of the interface. Control of this level was achieved with difficulty by careful adjustment of the rate of bottoms withdrawal.

All control was manual. External streams were moved smoothly through Tygon tubing by means of a multichannel finger pump. The column was operated at 25° C. Steady state was generally achieved within 5 hours.

The bottoms, tops, and reflux flow rates were measured by timing collections in calibrated burets or funnels. Solute concentrations in the bottoms and tops were measured with a Beckman DU spectrophotometer.

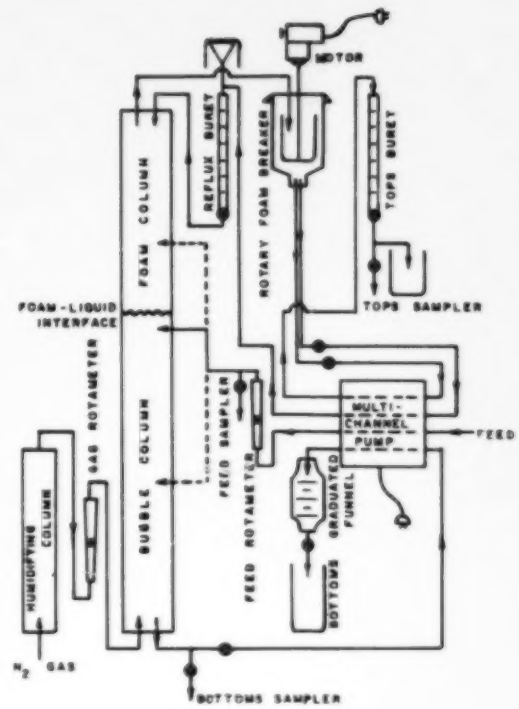

Figure 1. Apparatus

Not to scale

Results

The over-all and solute material balances are, respectively,

$$W + D = F \tag{1}$$

and

$$WC_W + DC_D = FC_F \tag{2}$$

Defining reflux ratio in the conventional manner of $(Q - D)/D$, and combining with Equations 1 and 2, yield

$$\left(\frac{W}{F}\right)\left(\frac{C_W}{C_F}\right) + \frac{Q}{(R+1)F}\left(\frac{C_D}{C_F}\right) = 1 \tag{3}$$

C_W/C_F is defined as the "stripping ratio" and decreases from unity to zero as the quality of stripping is improved. C_D/C_F is defined as the "enrichment ratio" and increases from unity as the quality of enrichment improves.

With the feed entering just below the interface between the two column sections, Figures 2 and 3 show the stripping performance and the enriching performance, respectively, and outline in a general way the configuration for the limits of column operability.

Figures 2 and 3 show that the performance is analogous in some ways to the more conventional techniques of separation, such as distillation. For example, raising the reflux ratio improves the quality of enrichment by bringing the rising foam in contact with rich downcoming liquid. Also, drawing off more overhead or more bottoms decreases the quality of enrichment or stripping, respectively. However, since surface phenomena are involved here, there are naturally certain special features too. The effect of gas flow rate is one of these.

At low gas rates, the few bubbles rising cause very little stripping. On the other hand, the foam produced rises slowly, draining well (A) and yielding a high enrichment. Thus, as G approaches zero, C_W/C_F approaches unity and $C_D \gg C_F$.

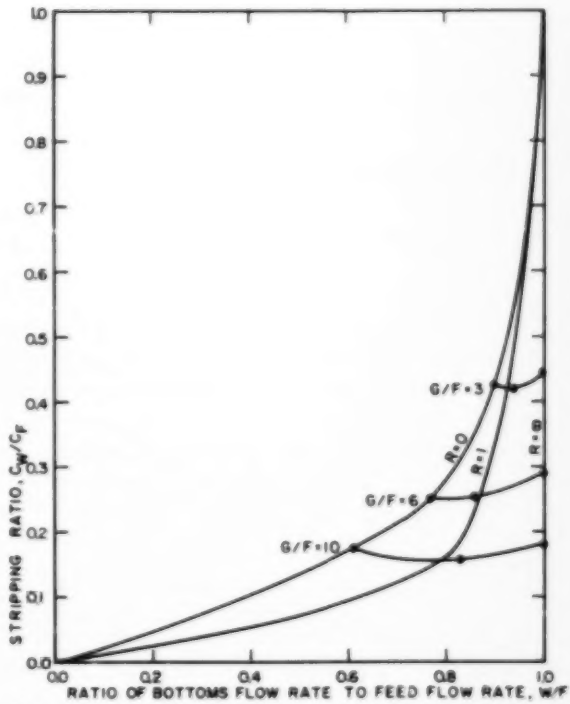

Figure 2. Stripping performance with feed entering near top of bubble column section

h = 105 cm. Decreasing ordinate represents improvement in degree of stripping

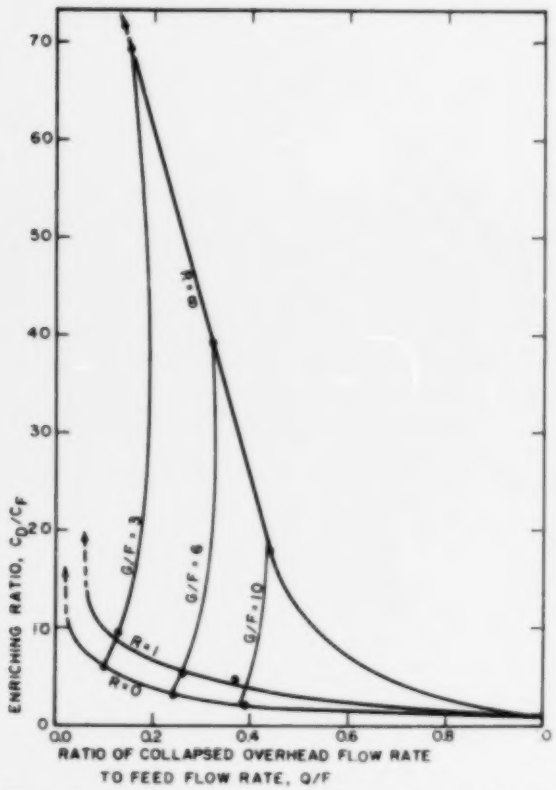

Figure 3. Enriching performance with feed entering near top of bubble column section

h = 105 cm. Increasing ordinate represents improvement in degree of enriching

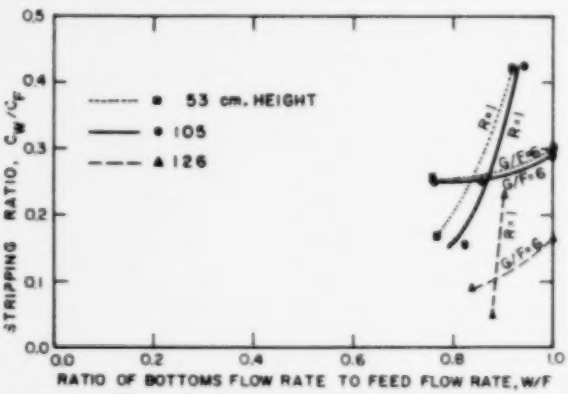

Figure 4. Effect of feed location on stripping performance

Data shown for R = 1 and G/F = 3, R = 1 and G/F = 10, R = 0 and G/F = 6, R = ∞ and G/F = 6. Decreasing ordinate represents improvement in degree of stripping

This argument fixes the upper right extremity of Figure 2 and confirms the trend towards the upper left in Figure 3.

At high gas rates the reverse is true. Strong stripping takes place because of large interfacial area presented by the many bubbles. However, much liquid is entrained in the rapidly rising foam, thus lowering the solute concentration in the overhead and yielding poorer enrichment. So as G becomes very large, C_W/C_F becomes very small and C_D/C_F approaches unity. This determines the lower left extremity in Figure 2

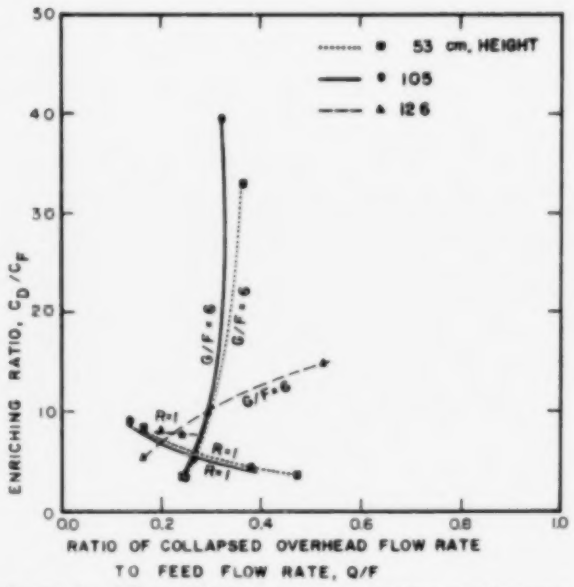

Figure 5. Effect of feed location on enriching performance

Data shown for R = 1 and G/F = 3, R = 1 and G/F = 10, R = 0 and G/F = 6, R = ∞ and G/F = 6. Decreasing ordinate represents improvement in degree of stripping

as the origin, and fixes the lower right extremity for C_D/C_F as unity in Figure 3.

Thus the results in Figure 2 show that stripping quality improves with increasing gas flow rate, while Figure 3 shows that enrichment quality improves with decreasing gas flow rate.

Lowering the feed inlet to a height of 53 cm., which is about midway up the bubble column, decreases the opportunity for bubble contact below the feed point and produces slightly poorer stripping, as shown in Figure 4. The slight extent of the effect here is attributed to virtual saturation of the bubble surfaces before their arrival at the feed location. (With a very low bulk concentration or a slowly adsorbed solute the effect should be more pronounced.)

Figure 4 also presents the effect of raising the feed inlet, in this case to a height of 126 cm. which is about one fourth the way up the foam column. Stripping improves markedly, indicating that much stripping takes place in the foam section below the feed inlet.

The effect on the enrichment of varying the feed location is presented in Figure 5. As with stripping, mentioned above, the effect on enrichment of lowering the feed inlet is slight. On the other hand, the effect of raising it is appreciable but somewhat complicated. Introducing the feed into the foam tends to make for a wetter (meaning a denser) foam than otherwise (*1*), with interstitial liquid of higher surfactant concentration. However, the improved stripping mentioned earlier means a lower concentration at the bottom, where the bubbles are formed. The bubble sizes are not uniform and their diameters increase with local surface tension (*1*), which itself increases as the bottom concentration decreases. The larger bubble sizes in turn make for less surface and better drainage in the foam, which then counters the aforementioned increased wetness. Furthermore, any significant change in the degree of bubble coalescence in the foam would be another complication. Thus the net effect on enrichment of raising the feed inlet up the foam column is difficult to predict *a priori*.

Conclusions

Combined bubble and foam fractionation operates successfully, with good stripping and enriching ratios obtainable. However, the incremental advantage of the elongated bubble section is small, at least for the present system.

Increasing the reflux ratio increases the degree of enrichment. Increasing the rate of gas flow improves the degree of stripping but decreases the degree of enrichment. Location of the feed inlet can be important under certain circumstances.

Nomenclature

C = solute concentration in liquid and collapsed foam streams, molarity
D = tops flow rate, ml./min.
F = feed flow rate, ml./min
G = gas flow rate, ml./min.
h = height above gas bubbler, cm.
Q = collapsed (air free) overhead flow rate, ml./min.
R = reflux ratio
W = bottoms flow rate, ml./min.

Subscripts
D = tops
F = feed
W = bottoms

Literature Cited

(1) Bikerman, J. J., "Foam," p. 2, Reinhold, New York, 1953.
(2) Brunner, C. A., Lemlich, R., *Ind. Eng. Chem. Fundamentals* **2**, 297 (1963).
(3) Lemlich, R., Lavi, E., *Science* **134**, No. 3473, 191 (1961).
(4) Leonard, R. A., Lemlich, R., *A.I.Ch.E. J.*, in press.
(5) Rubin, E. E., Gaden, E. L., Jr., "New Chemical Engineering Separation Techniques," H. M. Schoen, ed., Chap. 5, "Foam Separation," p. 319, Interscience, New York, 1962.

Received for review September 20, 1963
Accepted July 20, 1964

Work supported by U. S. Public Health Service Research Grant WP-161.

Printed in U. S. A.

A.I.Ch.E.—I.Chem.E. Meeting—London, 1965

Reprinted from the
Proceedings of the
Symposium on

New Chemical Engineering Problems in the Utilisation of Water

Reproduced from
best available copy.

A.I.Ch.E.—I.Chem.E.
Symposium Series No. 9

* 1965 A.I.Ch.E.—I.Chem.E. Symposium Series

The Proceedings of the A.I.Ch.E—I.Chem.E. Joint Meeting held in London, 13–17 June 1965 are being published in the 1965 A.I.Ch.E.—I.Chem.E. Symposium Series, each symposium forming a separate volume.

1 Advances in Separation Techniques

2 Chemical Engineering Under Extreme Conditions

3 Reaction Kinetics in Product and Process Design

4 Application of Mathematical Models in Chemical Engineering Research, Design, and Production

5 Materials Associated With Direct Energy Conversion

6 Transport Phenomena

7 Management Oriented Topics

8 Chemical Engineering Education (Published in *The Chemical Engineer*, September 1965)

9 New Chemical Engineering Problems in the Utilisation of Water

10 Mixing—Theory Related to Practice

Published by The Institution of Chemical Engineers, 16 Belgrave Square, London S.W.1
Price £3 ($9).

PREDICTING THE PERFORMANCE OF FOAM FRACTIONATION COLUMNS

By SATURNINO FANLO, B.S., Ph.D.*† and ROBERT LEMLICH, B.Ch.E., M.Ch.E.,P.E., Ph.D.*

SYNOPSIS

A procedure is outlined for predicting the performance of foam fractionation columns over a wide range of conditions. The method is based on theoretical considerations relating to adsorption at bubble interfaces and to drainage through randomly inclined capillaries of non-circular cross section with finitely viscous walls. Results are confirmed experimentally.

Introduction

During the past several years there has been a rise of interest in the technique of separating the components of liquid mixtures by means of foam fractionation. Studies reported include those of the present authors' group[1–4] as well as those of a number of other investigators. Of the latter, a representative few of the more recently reported studies are here cited[5–9] together with an extensive literature review[10] which appeared in 1962.

Much of the attention has been directed to aqueous wastes, including the removal of detergents and other pollutants from sewage, the separation of radioactive contaminants, and the treatment of pulping wastes. Most of the studies reported have been empirical in nature. Accordingly, the present authors have been concerned with elucidating the mechanism involved in the operation of foam fractionation columns in an effort to predict their performance from fundamental considerations.

Foam fractionation is based on the preferential adsorption of a solute at the interfaces of bubbles which are usually formed by deliberately sparging a liquid mixture with a gas. These bubbles rise, forming a foam which carries solute off overhead, thus effecting a partial separation of components.‡ After the foam which has been withdrawn overhead is allowed to collapse, a portion may be returned to the top of the column as deliberate reflux. This reflux then flows down through the foam filling the interstices with solution of higher concentration. This counter-current action enriches the rising foam, which increases the degree of separation.[2]

Prediction of Column Performance

Foam fractionation columns can be operated simply, or as strippers, enrichers, or combined columns.[2] Fig. 1 illustrates these four modes for continuous operation.

The foam bubbles are very nearly spherical when formed. Thus their ratio of surface to volume is $6/d$.§ However, in most systems they quickly drain to form blunted polyhedra. For uniform values of d_i, the foam bubbles can be assumed to be approximately regular dodecahedra,[11] for which configuration the ratio of surface to volume is $6{\cdot}59/d$.

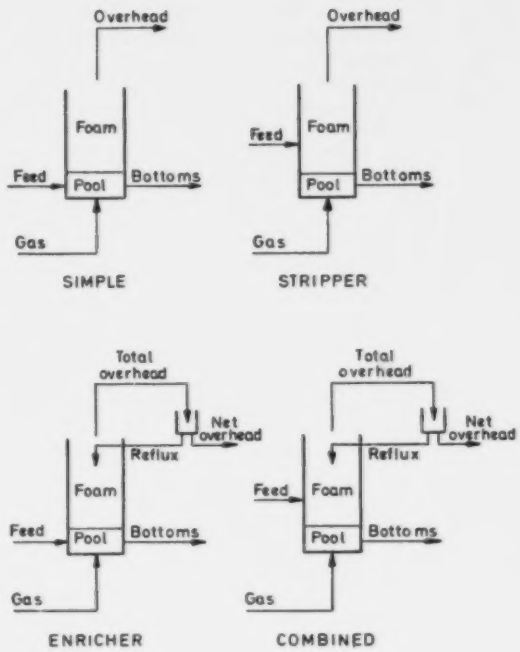

Fig. 1.—*Continuous foam fractionation columns illustrating four modes of operation*

The solute carried upward is largely in the bubble surfaces as surface excess, Γ, but it is also partly in the interstitial liquid. Combining this fact with overall material and solute balances, plus some lesser considerations relating to bubble distortion and drainage, we obtain equations (1)–(4) for columns operating without internal bubble coalescence.[4] For simple operation:

$$C_W = C_F - \frac{6G\Gamma}{Fd} \quad . \quad . \quad . \quad (1)$$

For stripping operations where the feed is some distance above the liquid pool:

$$C_W = C_F - \frac{6{\cdot}59G\Gamma}{Wd} \quad . \quad . \quad . \quad (2)$$

* Department of Chemical Engineering, University of Cincinnati, Cincinnati, Ohio 45221, U.S.A.

† *Present address:* Esso Research and Engineering Company, Florham Park, New Jersey, U.S.A.

‡ *Foam fractionation should not be confused with froth flotation. The latter operation, often used in the mineral industries, is a different technique. Froth flotation is employed to effect a solid-solid separation.*

§ *Symbols have the meanings given them on p.* 9:78

For enriching operations in a column which is tall enough to allow the concentration in the downcoming interstitial liquid to approach that in the rising interstitial liquid:

$$C_D = C_W + \left[6{\cdot}59 - \frac{0{\cdot}59}{R+1}\right]\frac{G\Gamma}{D'd} \quad . \quad (3)$$

For combined operation involving the qualifications of both equations (2) and (3) above:

$$C_D = C_F + \frac{6{\cdot}59G\Gamma}{D'd} \quad . \quad . \quad . \quad (4)$$

For bubbles of non-uniform size, d for the above equations should be calculated by equation (5):

$$d = \frac{\Sigma n_i d_i^3}{\Sigma n_i d_i^2} \quad . \quad . \quad . \quad . \quad (5)$$

The appearance of 6 rather than 6·59 as the coefficient in equation (1) stems from the notion that the incremental adsorption due to distortion (of spherical bubbles to dodecahedral bubbles after leaving the liquid pool) is only gained at the expense of solute in the interstitial liquid which is not replaced by any downcoming feed. A similar situation holds in part for equation (3).

Any coalescence (bubble breakage) in the column decreases the bubble surface in the column and decreases the rate of overhead flow. However, it also serves as internal reflux which enriches the rising foam. The derivations of equations (1)–(4) are predicated on the absence of coalescence. A small but significant degree of coalescence can easily go unnoticed by eye, especially in a foam of initially non-uniform bubble size. Coalescence is increased by decreasing the gas velocity which makes for a longer residence time and thinner (hence more fragile) bubble walls as a result of more complete drainage. For a moderate degree of coalescence, a value d averaged between the top and bottom of the column should be used.

In some cases Γ can be obtained from measurements of surface tension by use of the Gibbs adsorption equation.[12] Alternatively, it may be obtained experimentally with a standard separator.[1] It is in the nature of foams that Γ is usually substantially independent of the concentration of solute in the liquid.

In a continuously operating foam column, the drainage is primarily through the interconnecting network of capillaries (Plateau borders) that constitute the edges of the polyhedral bubbles. These capillaries are randomly oriented, with non-circular cross-section, and with non-rigid walls that tend to flow along with the drainage. By solving the differential momentum and material balances for a hydrodynamic model which includes these three important characteristics of capillaries, expressions were obtained[4] for predicting the foam density and, more important, the flow-rate, D.

For overhead form of relatively low liquid content leaving a vertical column:

$$B = J\frac{G^2\mu}{Ag\rho d_0^2} \quad . \quad . \quad . \quad (6)$$

where:

$$d_0^2 = \frac{\Sigma n_i d_i^3}{\Sigma n_i d_i} \quad . \quad . \quad . \quad . \quad (7)$$

and:

$$J = \phi\left(\frac{\mu^3 G}{\mu_s^2 g\rho A}\right) \quad . \quad . \quad . \quad (8)$$

Then:

$$D = B(1 + 3B/G) \quad . \quad . \quad . \quad (9)$$

The function ϕ depends somewhat on the particular boundary conditions selected to describe the complicated action in the foam during when it is being taken off at the very top of the column. Fig. 2 represents the current thinking of the present authors in this regard.[13]

The surface viscosity, μ_s, is a physical property. It can be estimated in several ways.[14, 15] Alternatively, and perhaps more suitably, it can be obtained from foam measurements for the particular system in question by using the equations above.

If moderate coalescence is present, the value of d_0 should be taken at the top of the column. For severe coalescence or highly non-uniform sizes of bubbles, the derivation of the above equations breaks down. A similar problem would arise in the event of marked deviation from plug flow for the bulk of the foam, as might occur in a column of varying or tortuous cross-section.

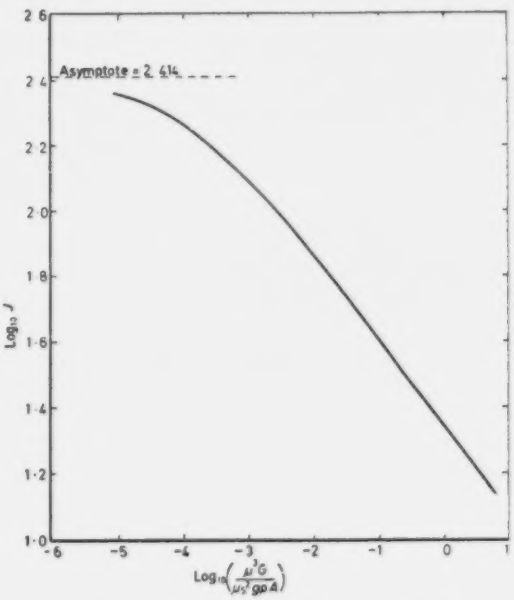

Fig. 2.—*Theoretical function for equation* (8).

An interesting result of the theory is that the density of the foam in the column is greater than D/G because of downward flow in the capillaries. Another is that the density in any one section of the column, such as between the reflux inlet and the feed, is uniform along the column. This somewhat startling result has been repeatedly confirmed experimentally provided that there was no coalescence.

Experimental Confirmation

The aforementioned theory has been supported by experimental results obtained in three separate laboratory columns of fairly straightforward construction.[1, 4] To further test the theory a more elaborate column was built incorporating electrodes to measure the electrical resistance of the foam and thus its density *in situ*.[13] The diameter of the bubbles was about 1 mm. The use of a metal spinneret as the bubbler yielded a fairly uniform size of bubbles for each run. However, the actual distribution of sizes was determined photographically. The system consisted of the non-ionic surfactant Triton X-100 ($C_8H_{17}-\phi-(OCH_2CH_2)_{9\cdot7}-OH$), the electrolyte sodium chloride, and water. Tests showed the small concentration of sodium chloride did not significantly affect the foaming for non-coalescing foam. Fig. 3 shows the apparatus.

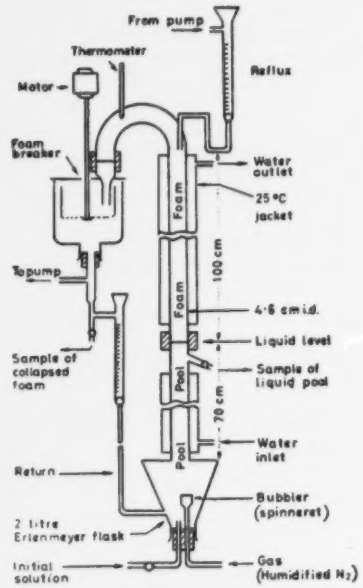

Fig. 3.—Foam fractionation column equipped for reflux and return. Seven pairs of electrodes (not shown) are distributed along the vertical column to measure the foam density by way of electrical conductivity. An eighth pair of electrodes is located past the overhead bend near the outlet

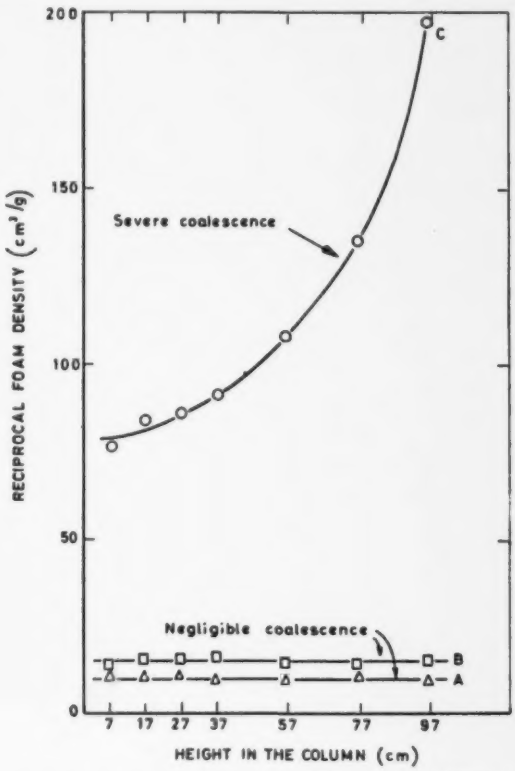

	Curve A	Curve B	Curve C
R	12·8	0	0
G (cm³ s)	9·6	9·6	1·7
d_0 (cm)	0·096	0·099	0·099
C_w (g mole/cm³)	$5·0 \times 10^{-7}$	$20·1 \times 10^{-7}$	$19·6 \times 10^{-7}$

Fig. 4.—Typical density measurements within the vertical foam column

Measurements of electrical resistance along the column, such as illustrated in Fig. 4, reconfirmed the uniformity of density when coalescence is absent, but at somewhat higher values than those predicted by theory. More importantly however, the experiments generally confirmed the equations listed above for predicting the performance of the column in the absence of severe coalescence.

This confirmation was further checked using rotary wiping blades instead of a U-bend for taking off the overhead flow. The manner of take-off was thus shown to be of relative unimportance. The results indicated a value of μ_s for Triton X-100 of about $0·8 \times 10^{-4}$ dyn s/cm, but it varied significantly with the concentration of the solute in the liquid. This is shown in Fig. 5. This value agrees fairly well with a value of μ_s of $1·0 \times 10^{-4}$ dyn s/cm determined independently by timing the rate of rise of thin black spots in bubble faces (of somewhat uncertain interstitial solute concentration but about 10^{-6} g mole/cm³) draining at unsteady state.[4] A value of Γ averaging about $2·8 \times 10^{-10}$ g mole/cm² was obtained, which also agrees with previous determinations[4] from foam and from Gibbs' equation.

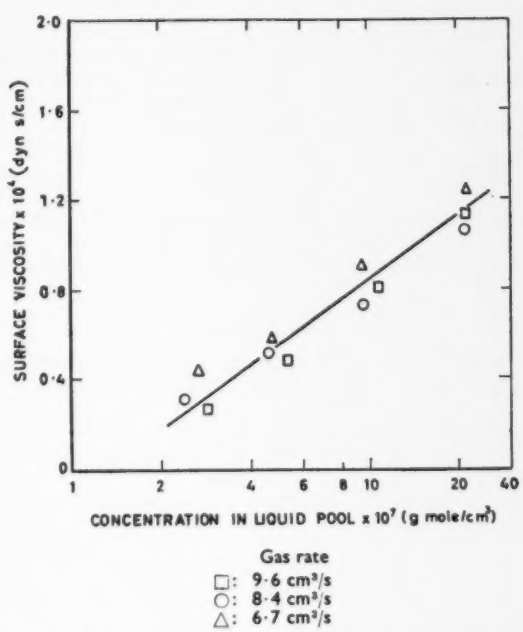

Fig. 5.—The surface viscosity of Triton X-100 determined with a U-bend take-off in the absence of severe coalescence within the column

Mass Transfer Considerations

Equations (3) and (4) were confirmed by experiment at low reflux ratios. However, at high reflux ratios the column was found to be too short to qualify as "tall enough" for the application of equations (3) and (4). Thus at high reflux ratios equations (3) and (4) represent the limiting situation. The extent to which the actual situation falls short of the limit depends on the hindrance to mass transfer between the upward and downward flowing interstitial liquid.

The mass transfer coefficient was determined experimentally with the present system and column. The coefficient is arbitrarily based on the wall area of the capillaries, and is pre-

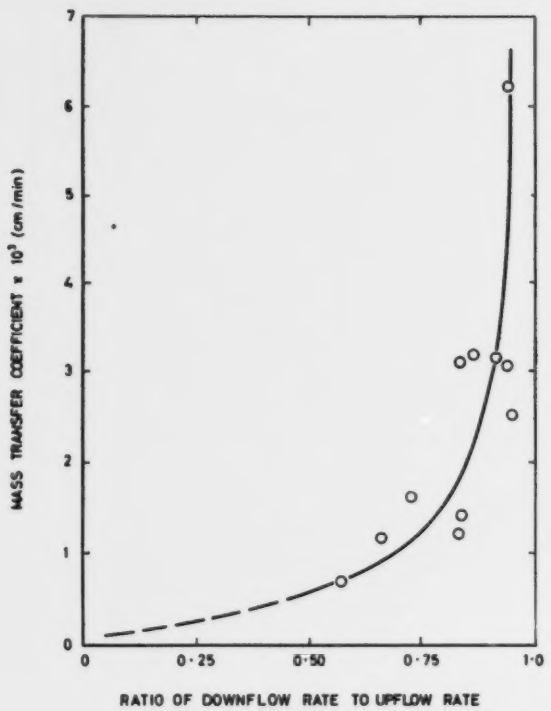

Fig. 6.—*Mass transfer coefficients*

sumed to be uniform over the length of the column. This analysis yields equation (10):

$$k = \frac{NU}{aD} \ln \frac{6{\cdot}59\,G\Gamma R}{[6{\cdot}59\,G\Gamma - Dd(C_D + \Delta C_L - C_W)](R+1)} \quad . \quad (10)$$

Both the upflow and downflow include internal recycle which can be estimated by means of the theory referred to earlier. The small effect of the aforementioned bubble distortion on the concentration in the interstitial liquid near the bottom of the foam is given by equation (11):

$$\Delta C_L = 0{\cdot}59\,\frac{G\Gamma}{Ud} \quad . \quad . \quad . \quad (11)$$

Fig. 6 shows typical values of the mass transfer coefficient so determined. Naturally, caution must be exercised in extrapolating these coefficients to other systems or conditions.

Symbols Used

A = horizontal cross sectional area of the column (cm²).
a = surface area of the walls of all the capillaries in the column (cm²).
B = quantity evaluated from equation (6) (cm³/s).
C_D = concentration of solute in the overhead flow on a gas-free basis (g mole/cm³).
C_F = concentration of solute in the feed (g mol/ecm³).
C_L = concentration of solute in the interstitial liquid near the bottom of the foam (g mole/cm³).
C_W = concentration of solute in the bottoms (g mole/cm³).
D = volumetric flow-rate of the overhead foam on a gas-free basis (cm³/s).
D' = $D/(R+1)$ = volumetric flow-rate of the collapsed (gas-free) net overhead product withdrawn when reflux is employed (cm³/s).
d = diameter of bubble averaged by volume and surface (cm).
d_i = individual bubble diameter (cm).
d_0 = diameter of bubble averaged by volume and diameter (cm).
F = volumetric flow-rate of feed (cm³/s).
g = gravitational acceleration (cm/s²).
G = volumetric flow-rate of gas (cm³/s).
J = quantity evaluated from equation (8).
k = mass transfer coefficient (cm/s or cm/min).
N = volumetric rate of interstitial liquid downflow (cm³/s or cm³/min).
n_i = number of bubbles with diameter d_i in a population of bubbles.
R = reflux ratio.
U = volumetric rate of interstitial liquid upflow (cm³/s).
W = volumetric flow rate of bottom product (cm³/s).
Γ = surface excess of adsorbed solute (g mole/cm²).
Δ = change in any property.
μ = liquid viscosity (dyn s/cm²).
μ_s = surface viscosity (dyn s/cm).
ρ = liquid density (g/cm³).
Σ = summation over a population of bubbles.
ϕ = function.

References

[1] Brunner, C. A. and Lemlich, R. *Industr. Engng Chem.* (*Fund.*), 1963, **2**, 297.
[2] Harper, D. O. and Lemlich, R. *Industr. Engng Chem.* (*Proc. Des. and Dev.*), 1965, **4**, 13.
[3] Lemlich, R. and Lavi, E. *Science*, 1961, **134**, No. 3473, p. 191.
[4] Leonard, R. A. and Lemlich, R. *A.I.Ch.E. Journal*, 1965, **11**, 18.
[5] Haas, P. A. and Johnson, H. F. *ORNL*—3527/1964. (Washington: United States Atomic Energy Commission.)
[6] Grieves, R. D. and Wood, R. K. *A.I.Ch.E. Journal*, 1964, **10**, 456.
[7] Klein, S. A. and McGauhey, P. H. *Journal of the Water Pollution Control Federation*, 1963, **35**, 100.
[8] Rubin, E. and Everett, R., Jr. *Industr. Engng Chem.*, 1963, **55**, No. 10, p. 44.
[9] Schoen, H. M., Rubin, E. and Ghosh, D. *Journal of the Water Pollution Control Federation*, 1962, **34**, 1026.
[10] Rubin, E., and Gaden, E. L. Jr. in Schoen, H. M. (Ed.). "*New Chemical Engineering Separation Techniques*," 1962, Chapter 5. (New York: Interscience Publications.)
[11] Bikerman, J. J. "*Foams: Theory and Industrial Applications*," 1953. (New York: Rheinhold Publications.)
[12] Osipow, L. I. "*Surface Chemistry: Theory and Industrial Applications*," 1962. (New York: Rheinhold Publications.)
[13] Fanlo, S. *Ph.D. Dissertation*, 1964. University of Cincinnati.
[14] Davies, J. T. and Rideal, E. K. "*Interfacial Phenomena*," 1961. (New York: Academic Press.)
[15] Mysels, K. J., Shinoda, K. and Frankel, S. "*Soap Films: Studies of their Thinning*," 1959. (Oxford: Pergamon Press.)

The manuscript of this paper was received on 26 October, 1964.

Mr. P. F. WACE asked two general questions about the use of reflux of foam columns as reported by Fanlo and Lemlich. Firstly, if the bubbles were spherical then for the same mean diameter as with dodecahedra the size of the flow channels would be larger, so that if throughput was important in the reflux operation he suggested that the use of a wetter foam containing spherical bubbles might be worth considering. Secondly, it looked as though there was a limit to the usefulness of reflux, which arose for a reason peculiar to foams. When refluxing a liquid containing a surfactant and an ion which had an affinity for that surfactant, it would be hoped that in the reflux section the surfactant would not be adsorbed on the bubbles (because there was already a monolayer of surfactant ions on their surfaces) but that the counter-ion would be further adsorbed. The concentration of the reflux liquid, however, was very likely to be above the critical micelle concentration for the surfactant, so that the extraction factor for the ion which it was desired to remove would be less than could otherwise be expected. Looking at the matter again, it might be better to use a wetter foam containing a more dilute liquid than a very dry dodecahedral bubble foam.

Dr. I. H. NEWSON said that with regard to equation (5) of the paper by Fanlo and Lemlich, he would like the authors to say what dimension of a regular dodecohedron was represented by the symbol d_t in that equation.

Turning to equation (3) of that paper:

$$C_D = C_W + \left[6{\cdot}59 - \frac{0{\cdot}59}{R+1}\right]\frac{G\Gamma}{D'd}$$

Dr. Newson said that he found it a most complex equation to derive, even with the answer in front of him, so that he would like to congratulate the authors on having conceived it in the first place. It seemed to him that the complexity in the equation stemmed from the fact that the authors had considered that the bubbles rising from the liquid pool at the bottom of the foam column were spherical, and then became deformed to regular dodecahedra because of draining in the foam section of the column. To account for that change of shape the term $0{\cdot}59/(R+1)$ was included in equation (3). In most cases however he imaged that R, the reflux ratio, was at least two, and possibly more, so that the value of the term $0{\cdot}59/(R+1)$ was at most 0·2. Since 0·2 was only 3% of 6·59 was it worth introducing that complexity into the equation when experimental spread was probably greater than 3%?

As a general comment on equations (2) and (3) of the paper, which dealt with injection of feed and/or reflux liquid into the foam phase, he noted from the early part of the paper that all experiments were in the region of surfactant bulk concentration where the surface excess, Γ, of the surfactant was constant. In that region the only benefit from reflux or foam feed operation would be due to the replacement of the comparatively dilute interstitial liquid with the more concentrated feed or reflux liquid. It was characteristic of most surfactants in solution that there was also a region where the surface excess, Γ, increased with bulk concentration, and in that region foam feed and reflux operation would not only provide enrichment of the interstitial liquid but would also increase the surface loading, increase Γ, of the air bubbles. Had the authors conducted any experiments in the region where surfactant surface excess varied with bulk concentration, and if so had they observed any striking differences between the values of enrichment obtained here compared with those obtained in the region of constant surface excess?

In equation (10) the authors had defined a mass transfer coefficient in terms of quantities which all appeared to be determined during the experiment; that referred to transfer between upward and downward flowing interstitial liquid. Dr. Newson felt that with that definition the mass transfer coefficient seemed to represent something more like a mixing coefficient, and in such a system a more orthodox mass transfer coefficient would refer to transfer between the interstitial liquid and the surfaces of the air bubbles.

As a matter of interest, the magnitude of the experimentally determined mass transfer coefficients, Fig. 6 on page 9: 78 it varied from 1 to 6×10^{-3} cm/min. From assessments based on measurements reported in the literature Dr. Newson felt that mass transfer coefficients between interstitial liquid and the surfaces of the air bubbles would be so

Mr. A. L. DOWNING said that in experiments at the Water Pollution Research Laboratory with a pilot plant for producing water of adequate quality for industrial use directly from sewage effluent, a foam separation unit was being used to remove the last traces of surfactants. The experience seemed to be that the concentration of surfactants of the alkyl benzene sulphonate type, such as were used in household synthetic detergents, could be reduced to about 0·5 ppm. To reduce the concentration further it would probably be necessary to use some kind of adsorption process.

Dr. LEMLICH, replying to Mr. Wace, said that the flow channels (interstices) below the reflux inlet automatically enlarged to accommodate the downflowing reflux. However, except for any effect on surface viscosity resulting from the increase in the surfactant concentration in the interstitial liquid, and of course barring bubble coalescence in the column, the use of reflux had very little effect on the drainage or wetness above the reflux inlet. Taking a well-drained foam of polyhedral bubbles off overhead made for a higher overhead concentration since the solute concentrates at the bubble surfaces. Reducing the quantity of interstitial liquid coming off overhead simply capitalises on the surface adsorption.

With regard to Mr. Wace's second question, Dr. Lemlich said that the use of reflux replaced interstitial liquid of relatively low concentration with that of much higher concentration. At high reflux ratios that made for an enormous increase in the degree of overall enrichment, as could be seen from equation (3) or equation (4) of the paper and the definition of $D' = D/(R+1)$. That had been confirmed experimentally.

Dr. Lemlich also said that his system involved only surfactant and water (except for a bit of inert electrolyte to give a reasonable conductivity for those runs where foam density was measured within the column). Thus his surface excess referred only to surfactant. Were a third substance present, its distribution coefficient between surface and interstitial liquid could indeed be affected adversely by the formation of micelles. However, the great cascading effect of reflux with its increase in the interstitial concentration of the third component might well override the change in distribution coefficient and yield a greater overall enrichment.

In reply to Dr. Newson, Dr. Lemlich said that d_t was the diameter of a sphere equal in volume to the regular dodecahedron. With regard to equation (3), he said that Dr. Newson correctly paraphrased the paper in describing the source of the bracketed coefficient. Dr. Lemlich also said that as an approximation this coefficient could be simply replaced by 6·3, since it varied only between 6·0 and 6·59 as R varied from 0 to infinity.

Dr. Lemlich said the surface excess of surfactant in a stable foam (or even a moderately unstable foam) was usually quite constant over a very large range of concentration in the liquid. No attempt was made to go beyond that range since at the lower limit the foam became too unstable and the upper limit (which is well above the critical micelle concentration) was far beyond the region of interest. Despite that constancy of surface excess, the continual replacement of some of the interstitial liquid with reflux of higher concentration could greatly increase the overall enrichment.

Dr. Lemlich said that in his experiments the bubble surfaces were saturated with surfactant so that the rate of mass transfer of surfactant to or from the surfaces was not a consideration. Thus comparison with such transfer rates reported in the literature was not valid. Rather, it was the rate of transfer between the upflowing and downflowing liquid streams which was important. Those streams were primarily in the capillaries. The magnitude of those internal streams were estimated by means of the original theory from externally measured quantities. For simplicity, the results were presented in terms of a convenient mass transfer coefficient. Alternatively, a mixing cell presentation or a transfer unit presentation could have been employed.

A STUDY OF INTERSTITIAL LIQUID FLOW IN FOAM

PART III: TEST OF THEORY

by

Fang-Shung Shih and Robert Lemlich

Department of Chemical Engineering
University of Cincinnati
Cincinnati, Ohio 45221

Notes: This section (constituting pp. 5-24) has been submitted to the A.I.Ch.E. Journal for publication. The figures, equations, and bibliographical references in this section are numbered independently of other sections.

Revised Manuscript, November 1966

Key Words: Foam -8, Interstitial Flow -8, Drainage -8, Overflow -8, Column -5, Theory -1,8, Model -1,8, Test -8,10, Experiment -1,10, Agreement -2, Fractionation -4, Separation -4, Prediction -4,8, Estimation -4,8.

ABSTRACT

The theory for foam drainage and overflow recently proposed by the present authors' group is tested with extensive experimental data gathered from foam fractionation columns and also from stationary foams at steady state. The experimental results appear to support the theory.

INTRODUCTION

Recently the authors' group presented a theory for foam drainage and overflow (7). It is based on interstitial Newtonian flow through randomly oriented capillaries (Plateau borders) of non-circular cross-section with surface viscosity at the capillary boundaries. It involves no empirical constants.

This theory permits the estimation of the rate at which foam flows off overhead from a foam fractionation column. Such columns are used to partially separate the constituents of liquid mixtures via differences in surface activity. Gas is bubbled up through a liquid pool at the bottom of the column, thus forming a foam which rises up the column and overflows the top. This overflow carries off solute which has been adsorbed at the bubble surfaces.

The degree of overhead enrichment, which may be considerable, can be increased even further through the use of internal or external reflux (3). The degree of stripping can be increased by injecting the feed into the foam some distance above the liquid pool (7). Figure 1 shows a foam fractionation column in these alternative modes of operation. The theory predicts the rate of

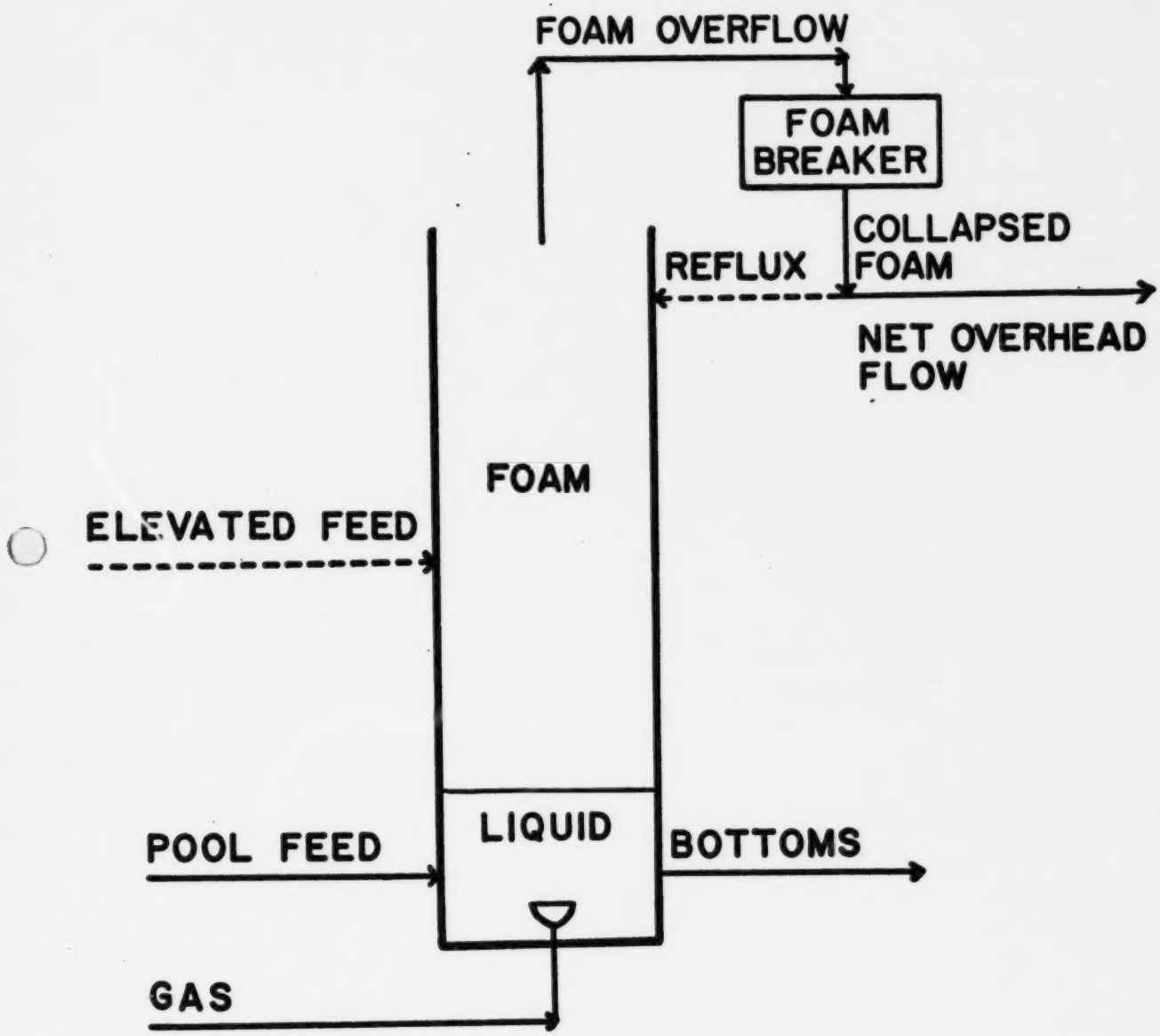

Figure 1. Four alternative modes of flow operation with a foam fractionation column. 1. Solid lines show the simple mode. 2. The dotted reflux line is for operation as an enricher. 3. For stripping operation, pool feed is replaced with elevated feed to the foam. 4. For combined operation, reflux and elevated feed are both employed.

foam overflow for all modes.

The theory incidentally also provides a relationship at steady-state between the bulk density of a stationary foam in a column and the rate of deliberate liquid feed draining through the foam keeping it moist. In this situation there is no pool feed and no gas flow, and therefore no foam overflow or reflux. There is only elevated feed, stationary foam up to the feed inlet (with empty column above it), and bottoms withdrawal. This is illustrated in Figure 2.

The theory has already been compared against limited experimental data (8). The purpose of the current paper is to present the results of a more extensive test. Details have been placed on file (10).

According to the theory (5,7) the rate of overhead flow for a fairly dry foam (meaning a foam of low liquid content) is given by Equation 1.

$$D = \frac{G^2 \mu}{Ag\rho d^2} \phi\left(\frac{\mu^3 G}{\mu_s^2 g \rho A}\right) \qquad (1)$$

The function ϕ was evaluated theoretically according to two alternatives regarding the detailed relationship between the interstitial downflow and the bulk foam upflow. The two evaluations are shown in Figure 3. The difference between them is minor, especially in the region of current interest.

Density ρ and viscosity μ are for the liquid in the capillaries. For dilute solutions these properties can be conveni-

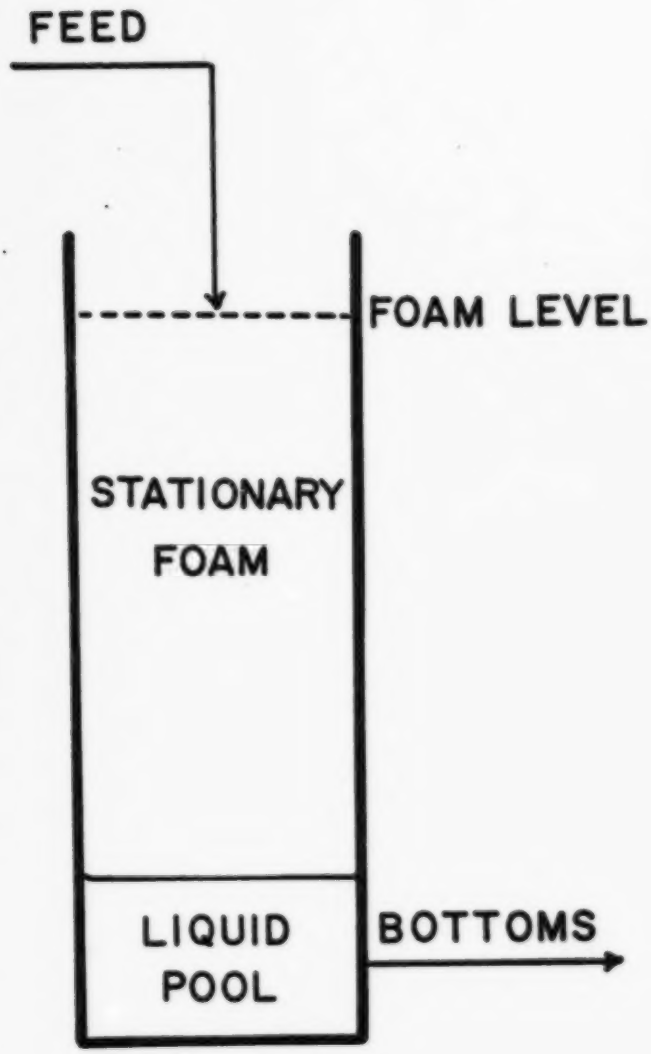

Figure 2. Steady state drainage through a stationary foam.

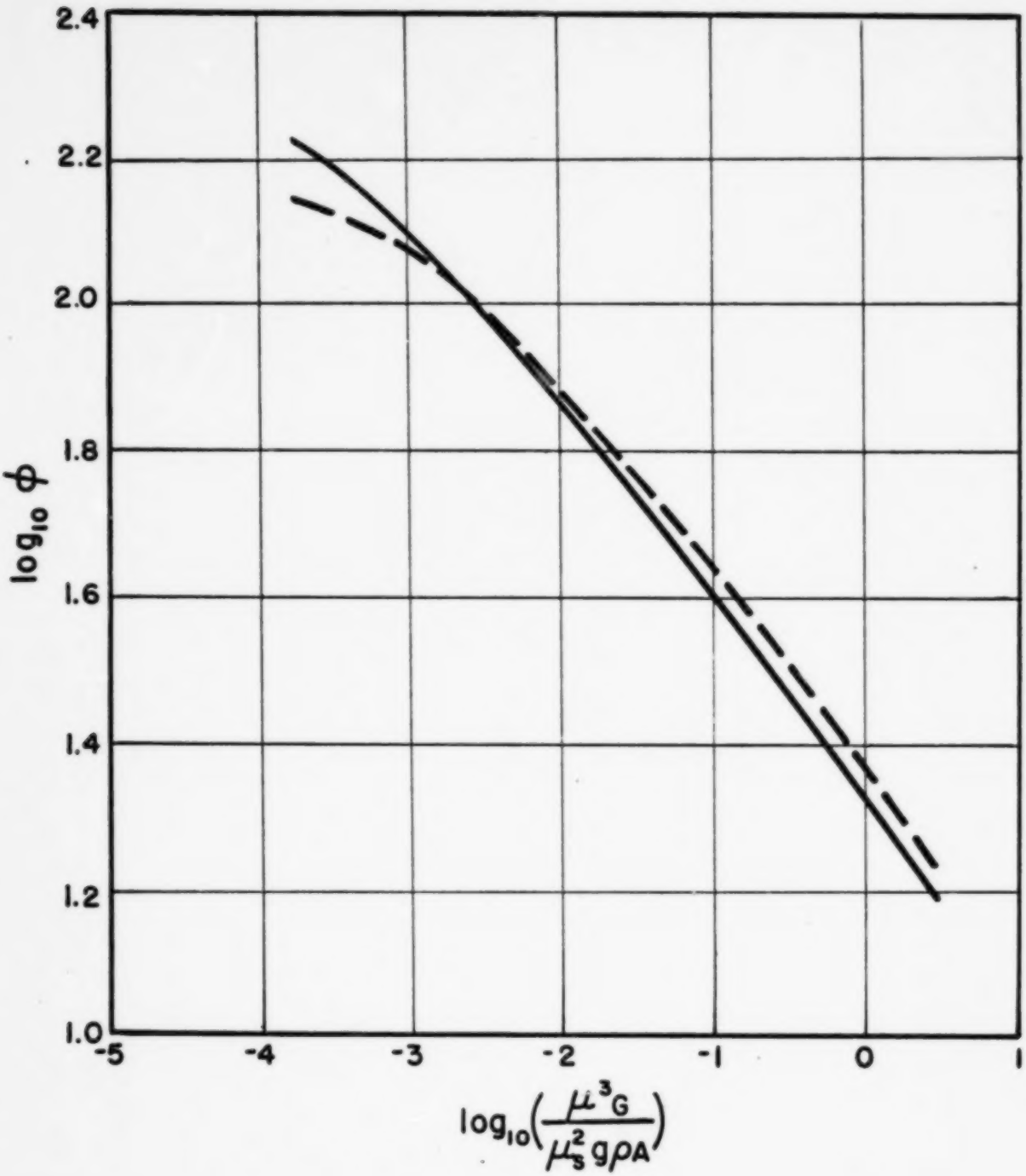

Figure 3. Theoretical evaluation of ϕ. The solid curve is based (4,5) on $v_{z,max,MO} = v_{f,SO}$. It has an asymptote of $\log_{10}\phi = 2.41$. The dashed curve is based (7) on $v_{z,max,MO} = \frac{3}{2} v_{f,SO}$. It has an asymptote of $\log_{10}\phi = 2.27$.

ently taken as those of the solvent which is usually water. Surface viscosity μ_s is a separate property which involves resistance to flow in a surface, as compared to μ which involves resistance to flow within a volume. Thus the dimensions of μ_s are force x time/length, while those for μ are of course force x time/area. The determination of μ_s is discussed later.

When there is appreciable variation in bubble diameter within the foam, an average d is employed according to Equation 2.

$$d^2 = \frac{\sum n_i d_i^3}{\sum n_i d_i} \qquad (2)$$

For foam of high liquid content, the theoretical procedure for estimating D is more complicated (7). However, if the foam has only a moderate liquid content and if ϕ falls within the substantially linear portion of Figure 3, then the complicated procedure can be greatly simplified into just multiplying D from Equation 1 by the quantity (1 + 3D/G) to give a corrected D. The interested reader is referred to the aforementioned earlier publications for further details.

If bubble coalescence is present within the foam column, d must be taken at the top of the column. This is important. Experiments conducted by the authors' group have shown that a small but very significant degree of coalescence can easily go unnoticed to the eye (5). It is also worth mentioning here that such coalescence furnishes internal reflux. Thus column operation which is nominally in the simple mode can in fact constitute opera-

tion in the enriching mode.

When d is not directly measured at the top of the column, it can be estimated from the average bubble diameter lower down the column by means of the ratio of corresponding bulk foam densities (7), should this ratio be known from measurement (4,5,8) or some other source.

For severe internal coalescence, highly non-uniform bubble sizes, or extremely high liquid content in the foam, the theoretical evaluation of ϕ breaks down since the model is based on flow through capillaries bounding regular polyhedral bubbles. For such cases, one can resort to an empirical evaluation of ϕ.

COMPARISON BETWEEN THEORY AND EXPERIMENT FOR FOAM OVERFLOW

Table 1 summarizes the data sources and results for the present test involving foam overflow. For the first three sets of data, the system employed was aqueous Triton X-100 with feed concentrations ranging from 4×10^{-7} to 20×10^{-7} g-mol/cc. Of course with reflux the range of interstitial concentrations was even greater. Triton X-100 is a commercial nonionic surfactant with the nominal formula $C_8H_{17}-C_6H_4-(OCH_2CH_2)_{9.7}-OH$.

For the first set of data, the column was operated in the simple mode. For the second set, 19 runs were conducted with the column operating in the simple mode, and the remaining 12 runs were conducted with external reflux in order to deliberately operate the column in the enriching mode. For the third set, feed entered the foam rather than the pool so that operation

Set	Reference	Aqueous System	Feed Inlet	External Reflux Ratio	d cm.
1	(6,8)	Triton X-100	Pool	0	0.11 to 0.24
2	(4,5)	Triton X-100	Pool	0 to 12.9	0.10 to 0.22
3	(6,8)	Triton X-100	Foam	0	0.05 to 0.40
4	(2,3)	Aresket 300	Pool	0	0.042 to 0.046
5	(1)	Essentially NaDBS	Pool	0	0.055 to 0.071

Table 1. Range of data and results for the test of theory presented in Figure 4.

Table continued on next page ⟶

G cc/sec.	D cc./sec.	A sq.cm.	μ_s dyne sec./cm.	Number of Runs	Average Deviation, %
1.3 to 3.2	0.001 to 0.028	16.6	1.0×10^{-4}	5	16
1.7 to 9.6	0.002 to 0.305	16.6	1.0×10^{-4}	31	29
1.3 to 10.4	0.001 to 0.405	13.1 to 13.8	1.0×10^{-4}	10	25
1.5 to 1.7	0.20 to 0.38	2.8 to 9.1	1.8×10^{-4}	3	12
2.8 to 2.9	0.09 to 0.12	11.2	8.2×10^{-5}	10	13
				Total = 59	

Continuation of Table 1.

was in the stripping mode.

Some of the early experiments (6) which yielded this third set of data involved very large slugs of gas in the foam and a very uncertain d at the top of the columns. Such runs are not included here.

The fourth set of data is for aqueous Aresket 300 (commercial monobutyl biphenyl sodium monosulphonate) with feed concentrations ranging from 8×10^{-7} to 16×10^{-7} g-mol/cc. This set of early results is very small due to the fact that most of the data from which the set is drawn are unusable here. This is because for this data the bubble diameter was not determined at the top of the column and there was a considerable but undetermined degree of internal coalescence for all runs. The small set selected here constitutes those runs for which coalescence seemed the least, and furthermore represents D data extrapolated to zero column height (zero residence time) to further minimize the effect of coalescence.

The fifth set is from the work of another group of investigators who used aqueous sodium dodecyl benzene sulphonate in the range of 1.5×10^{-7} to 2.6×10^{-7} g-mol/cc in the presence of trace radioactive ions. Their photographs seem to show a wider range of bubble sizes within each bubble population than was usually the case for the authors' group of investigators who strove by means of special spargers to achieve more uniform bubble sizes within each run. Accordingly, with small bubbles fitting between larger bubbles, for a given bulk foam density their bubbles can be ex-

pected to have been more nearly spherical (and hence less polyhedral) than those of the authors' group. Their photographs seem to confirm this. There is also the question of internal coalescence in their foam. Nevertheless, for the sake of completeness their data are included in the present test.

The detailed bubble data required for applying Equation 2 to this fifth set was not published. Accordingly, d was obtained by dividing the spherical geometric factor 6 by their published values of average specific bubble surface. This does not give quite the same results as Equation 2 but is the best that can be done with the information available.

The surface viscosity for the first three sets of data; that is, for aqueous Triton X-100, has been measured independently (8) by the black spot method of Mysels (9). Its value was found to be 1.0×10^{-4} dyne sec./cm. at 25°C.

Unfortunately, no μ_s measurements are known to the present authors for the systems employed in the last two data sets. Accordingly, for these two sets, μ_s was determined by applying the theory to the foam data. This was accomplished by combining Equation 1 with the wetness factor (1 + 3D/G) and the solid curve of Figure 3, and then substituting for the quantities involved so as to solve for μ_s for each run. Results were then averaged. This yielded a μ_s of 1.8×10^{-4} dyne sec./cm. for the aqueous Aresket 300 and 8.2×10^{-5} dyne sec./cm. for the aqueous NaDBS. Naturally, values of μ_s so determined incorporate not only any error

in the data but also any deficiencies in the foam theory. On the other hand, they naturally improve the theoretical estimation of D over what might be expected from independently measured values of μ_s.

For the first four sets of data, the temperature was 25°C. Conditions for the fifth set were apparently near ambient too. Accordingly, for all five sets, μ is taken as 8.94×10^{-3} dyne sec./cm^2, ρ as 1.00 g/cc, and g as 980 cm/sec^2. There is evidence which indicates that μ_s, at least for Triton X-100, can vary markedly with temperature (4,5). Impurities can also affect μ_s.

Figure 4 shows the test. The ordinate represents D/A calculated from theory; that is, from Equation 1, the wetness factor (1 + 3D/G), and the solid curve of Figure 3. (Use of the dashed curve of Figure 3 would have yielded nearly the same results.) The abscissa of Figure 4 represents experimental values of D/A. The diagonal is the line of theoretical perfection.

Examination of Figure 4 reveals reasonably good agreement between the plotted points and the theoretical line. The average deviation of theory from experiment is listed in Table 1 for each set of data. The average deviation is 26% for the points involving the independently measured μ_s, and 23% for all the points. In view of the wide range of variables covered (more than 1000-fold for D/A) and the experimental difficulties involved, this is deemed to be good agreement between theory and experiment.

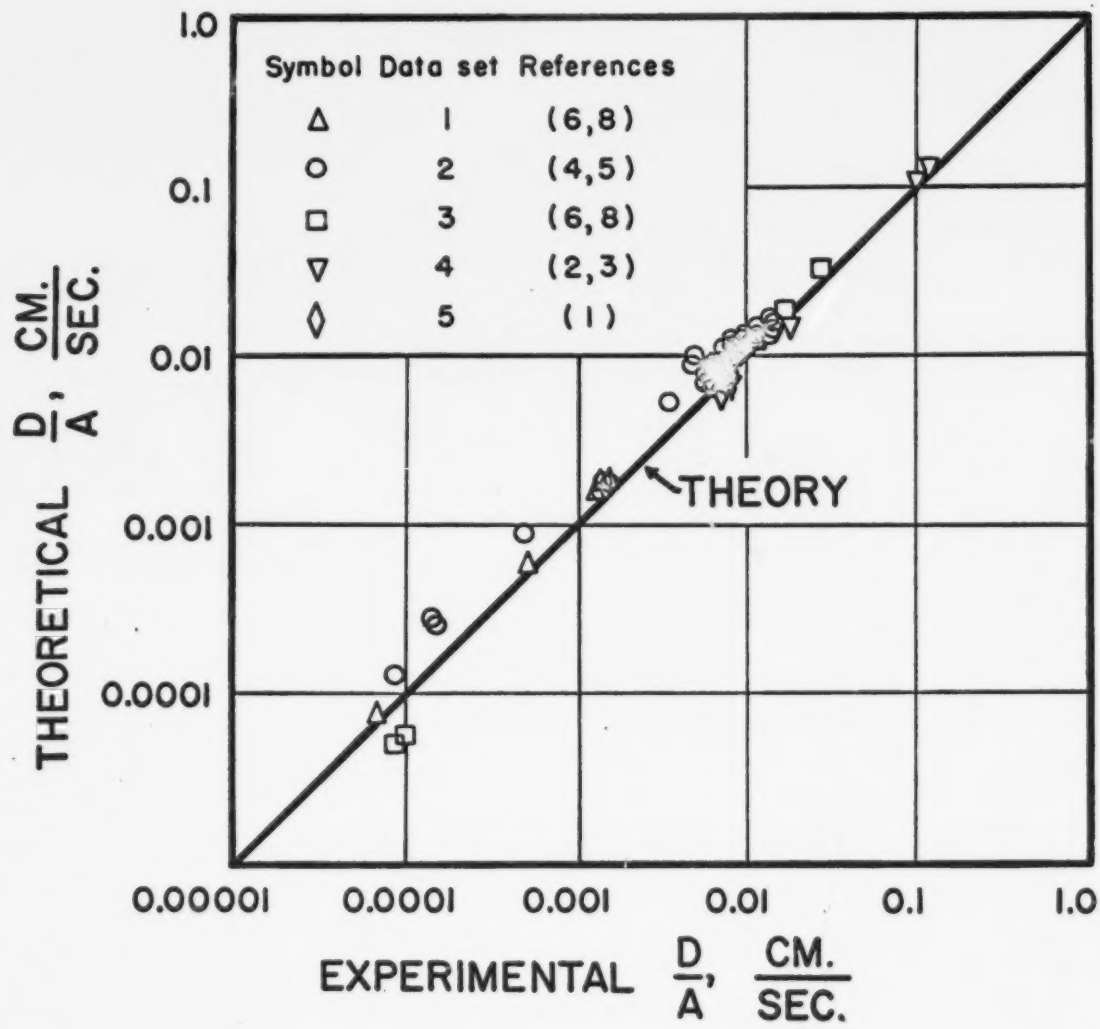

Figure 4. Test of theory (5,7) for predicting the foam overflow rate. Data set numbers refer to Table 1.

Of course the agreement can be improved further by using foam determined μ_s for the first three sets of data as well. In this connection, the apparent effect of concentration in the interstitial liquid on μ_s, as exhibited in Figure 5 of reference (5), can be incorporated. However, this would reduce the independence of the test and so, for the sake of maximum objectivity, has not been done here.

COMPARISON FOR STEADY STATE DRAINAGE

As mentioned earlier in the Introduction, the theory also furnishes a theoretical steady-state relationship between the bulk density of a stable stationary foam trapped in a column and the rate of a liquid stream fed on to the top of the foam so as to drain through to the bottom.

In this connection, two sets of experimental data are available to test the drainage theory. For the first set (6,8) d was 0.37 cm and A was 13.1 cm^2, while for the second set (4,5) d ranged from 0.10 to 0.19 cm and A was 16.6 cm^2. Aqueous Triton X-100 was employed for both sets. Accordingly, the independent μ_s value of 1.0×10^{-4} dyne sec./cm. is used here for the test. The temperature was 25°C. Since the foam was stationary, G of course was zero.

Figure 5 shows this drainage test. The ordinate represents the drainage rate predicted by theory from the measured bulk foam density and other pertinent information. This theoretical drainage rate was calculated according to the information flow diagram

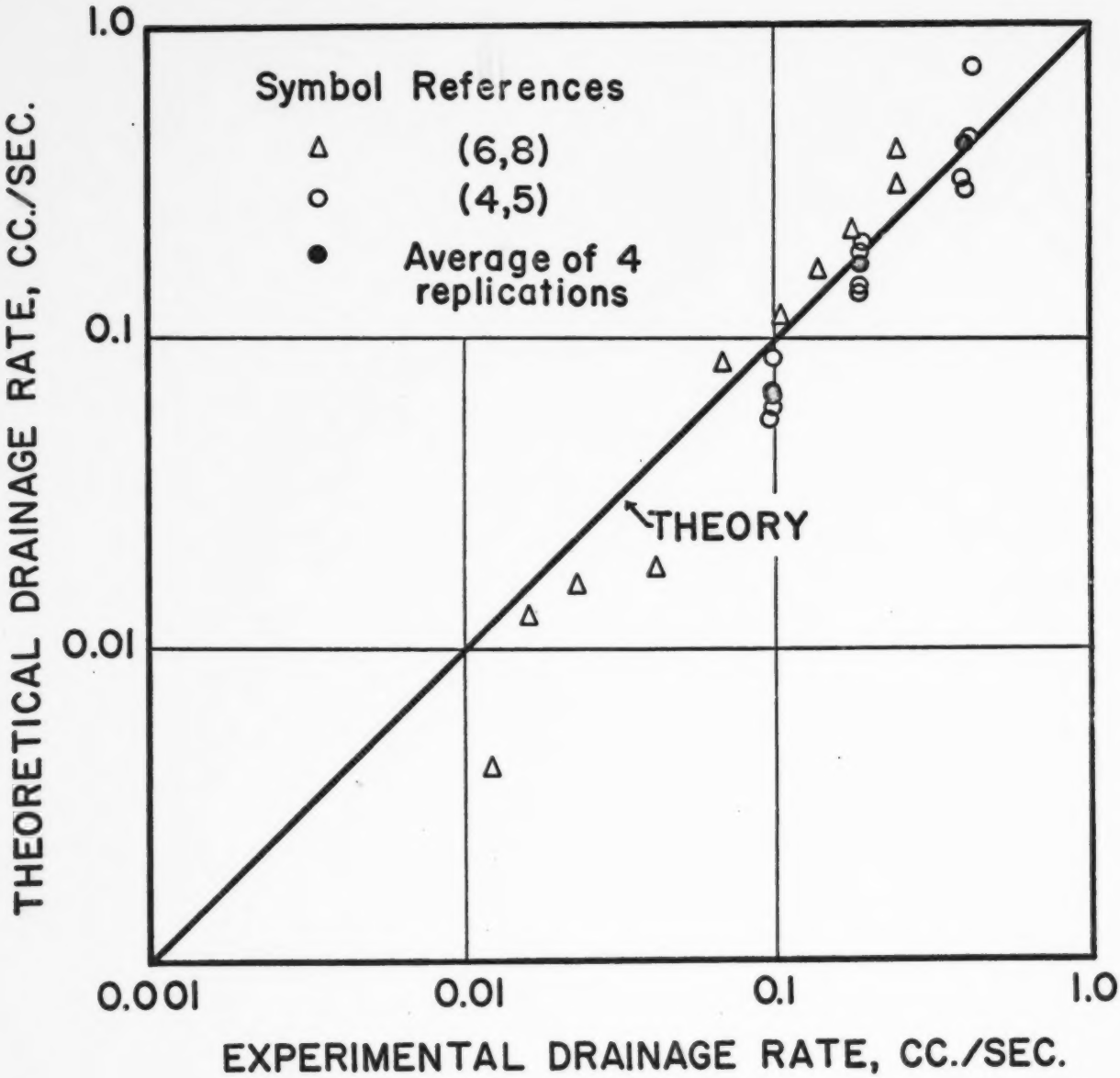

Figure 5. Test of theory (7) for predicting the rate of steady state drainage through a stationary foam.

of Figure 6 in which all notation, equation numbers, and figure numbers refer to reference (7). The aforementioned function ϕ does not enter the calculation in any way. Input information is encircled. Input t is of very small effect here. It was determined from Figure 5 of reference (8) but could just as well have been neglected.

The abscissa of Figure 5 represents the experimentally measured drainage rate. As before, the diagonal is the line of theoretical perfection. Inspection of this figure reveals fair agreement except at the lower drainage rates where experimental error is likely to be greatest. The average deviation of theory from experiment is 29%.

If one considers the experimental scatter apparent in the three sets of quadruplicated runs (shown as open circles in Figure 5), and then compares the three corresponding averages against the diagonal (so as to minimize the effect of individual error), better agreement between theory and experiment becomes immediately evident. The average deviation for these three averages is only 18%.

In view of the range of variables, the experimental difficulties, and the use of the independently determined value for μ_s, the test represented in Figure 5 appears to yield fair agreement between theory and experiment.

CONCLUSIONS

The experimental results appear to support the theory. This is especially evident in light of the wide range of variables in-

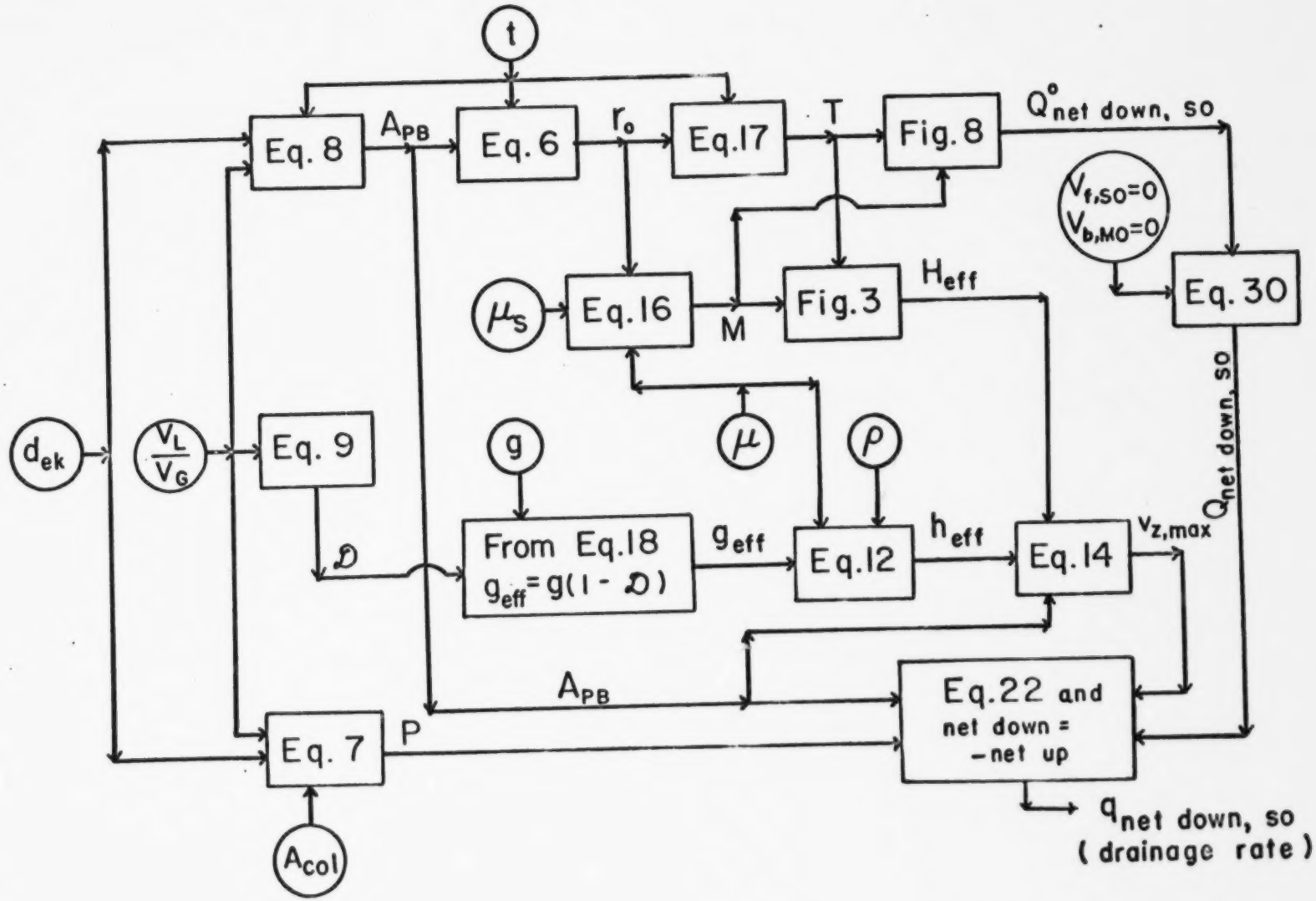

Figure 6. Information flow diagram for predicting from theory (7) the rate of steady state drainage through a stationary foam. Input information is encircled. Since $v_{f,SO} = 0$ and $v_{b,MO} = 0$, BO = MO = SO. Notation, equations, and figures refer to reference (7).

volved. Over more than a 1000-fold range of overflow rate, the average deviation of theory from experiment is only 26%, even with μ_s independently determined.

ACKNOWLEDGMENT

This work was supported by U. S. Public Health Service Research Grant WP-00161.

NOTATION

A	horizontal cross sectional area of a foam column, sq.cm.
D	volumetric flow rate of the entire foam overflow on a gas-free basis, cc./sec.
d	average bubble diameter, cm.
d_i	individual bubble diameter, cm.
G	volumetric flow rate of gas, cc./sec.
g	gravitational acceleration, cm./sec^2.
n_i	number of bubbles with diameter d_i.
t	interstitial film (face) thickness, cm.
$v_{f,SO}$	upward velocity of the aggregate of foam bubbles relative to a stationary observer, cm./sec.
$v_{z,max,MO}$	maximum velocity downward within a vertical capillary relative to the aggregate of foam bubbles, cm./sec.
$\bar{v}_{z,max,MO}$	average velocity downward within a vertical capillary relative to the aggregate of foam bubbles, cm./sec.

Greek Letters

μ	liquid viscosity, dyne sec./sq.cm.
μ_s	surface viscosity, dyne sec./cm.
Φ	function
ρ	liquid density, g./sec.

LITERATURE CITED

1. Banfield, D. L., I. H. Newson, and P. J. Alder, A.I.Ch.E.-I.Chem.E. Symposium Series (London) 1, in press (1965). Also private communication.

2. Brunner, C. A., Ph.D. dissertation, University of Cincinnati, Cincinnati, Ohio (1963).

3. _____, and R. Lemlich, Ind. Eng. Chem. Fundamentals, 2, 297 (1963).

4. Fanlo, S., Ph.D. dissertation, University of Cincinnati, Cincinnati, Ohio (1964).

5. _____, and R. Lemlich, A.I.Ch.E.-I.Chem.E. Symposium Series (London) 9, 75 (1965).

6. Leonard, R. A., Ph.D. dissertation, University of Cincinnati, Cincinnati, Ohio (1964).

7. _____, and R. Lemlich, A.I.Ch.E. Journal, 11, 18 (1965).

8. Ibid., 11, 25 (1965).

9. Mysels, R. J., K. Shinoda, and S. Frankel, "Soap Films, Studies of their Thinning", Pergamon Press, New York (1959).

10. Shih, F. S., Ph.D. dissertation, University of Cincinnati, Cincinnati, Ohio, in preparation.

UNSTEADY DRAINAGE THROUGH A STATIONARY FOAM*

by

David W. Drott and Robert Lemlich

*Notes: This is not yet a completed paper for publication. Figures, equations, and bibliographical references are numbered here independently of previous sections.

SUMMARY

The theory which was developed earlier for interstitial flow through foam should, in principle, be adaptable to the important problem of unsteady drainage from a standing foam, provided bubble coalescence in the foam is either negligible or accountable. Accordingly, the problem was attacked by combining the interstitial flow theory with a differential material balance and suitable boundary conditions. The combination was then solved in dimensionless form via finite differences with an I.B.M. 1620 digital computer to give a typical history for the foam density at an arbitrary height in the draining foam.

The theoretical density history so obtained was then compared against an experimentally measured history for a standing foam of aqueous Triton X-100, which is a commercial nonionic surfactant. The experimental density was determined by measurement of electrical conductivity using the apparatus described in the paper by Fanlo and Lemlich (1) which constitutes an earlier part of the present Progress Report.

The comparison between theory and experiment revealed that coalescence was of overriding importance in the unsteady drainage of Triton X-100. Whether or not this would also be so in more stable foams is a matter for further investigation with other substances.

The matter of coalescence itself is also under further study. The aforementioned kind of comparison is one approach being employed in such study.

THEORY

Consider first a foam draining at steady state as shown in Figure 1. This represents the initial conditions within the foam. The interrelationships among the variables describing such a foam can be determined as indicated in the last figure of the paper by Shih and Lemlich (4) which constitutes an earlier part of the present Progress Report. Said figure in turn is based on the theory presented in the paper by Leonard and Lemlich (Part I) (2) which also constitutes an earlier part of the present Progress Report.

The initial conditions will be designated here by the subscript o. Unless specified otherwise, all symbols are defined in accord with the table of notation on the last page of the accompanying paper by Leonard and Lemlich (Part II) (3).

The feed is now shut off and the foam allowed to drain in unsteady state, as shown in Figure 2. A mass balance is taken over a differential foam element shown in Figure 3. (Since liquid ρ is essentially constant, the more convenient liquid volume balance will be written instead.) This yields

$$-\frac{\partial q}{\partial x} = \frac{\partial}{\partial \gamma}(PA_{PB}) \qquad (1)$$

where x is the distance downward and q is the flow downward. Define the dimensionless quantities $\hat{q} = q/q_o$, $\hat{A} = A_{PB}/(A_{PB})_o$, and $\hat{P} = P/P_o$. Also define $X = x/L$ and $\hat{T} = \frac{q_o \gamma}{P_o (A_{PB})_o L}$, where L is the height of foam. Com-

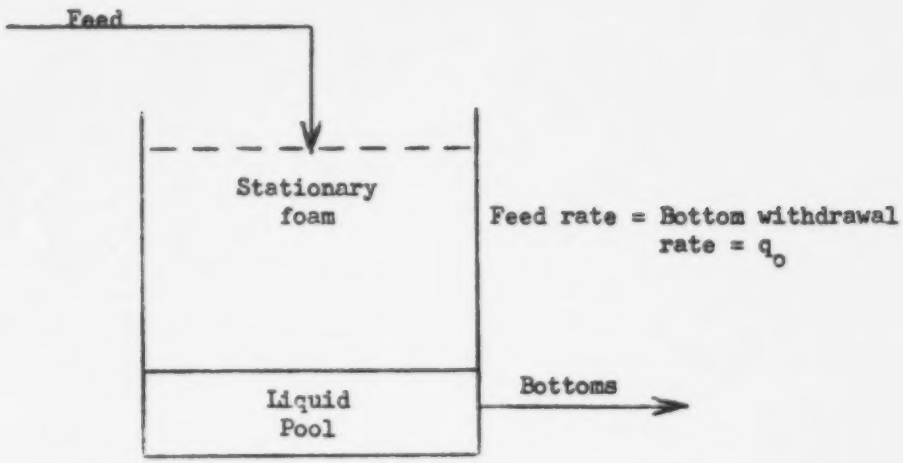

Figure 1. Steady state drainage through a stationary foam. This represents the initial conditions.

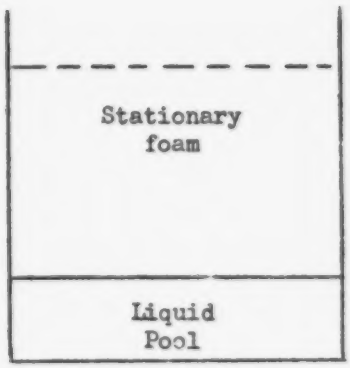

Figure 2. A stationary foam draining in unsteady state. Interstitial liquid drains down to the liquid pool. No feed is supplied to make up for the depletion.

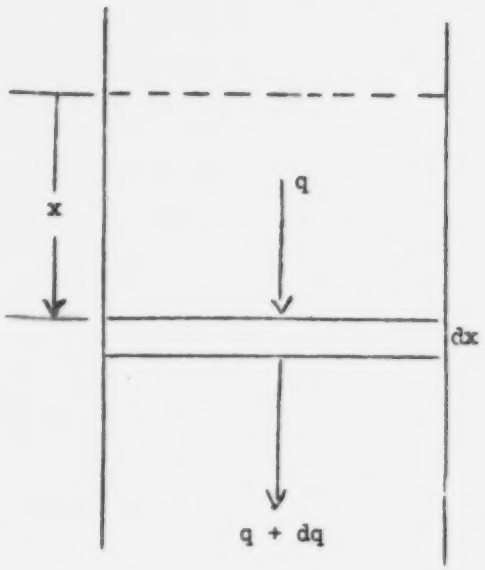

Figure 3. Differential element in a foam column, taken for purposes of material balance.

bining these five definitions with Equation (1) yields Equation (2).

$$-\frac{\partial \hat{q}}{\partial X} = \frac{\partial}{\partial \hat{T}} (\hat{P}\hat{A}) \tag{2}$$

Define $R = r_o/(r_o)_o$. For a draining foam, $t << r_o$. Then, from Equation 6 of reference (2),

$$\hat{A} = R^2 \tag{3}$$

Also, $t << d_{32}$. Then, from Equation 8 of reference (2), the definition of $\hat{A}$ and the new definition $Z = V_L/V_G$,

$$Z = E\,\hat{A} \tag{4}$$

where

$$E = \frac{60\ (A_{PB})_o}{2.445\pi d_{31}^2} \tag{5}$$

Combining Equations (3) and (5),

$$Z = E\,R^2 \tag{6}$$

From Equation 7 of reference (2) and the definition of P and Z, and neglecting any changes in d_{31},

$$\hat{P} = \frac{1 + Z_o}{1 + Z} \simeq 1 \tag{7}$$

Thus Equation (2) can be simplified to

$$\frac{\partial \hat{q}}{\partial X} = -\frac{\partial \hat{A}}{\partial \hat{T}} \tag{8}$$

Equation 18 of reference (2) can be here expressed as

$$g_{eff} = g(1 - \mathcal{S}) - \frac{\gamma}{\rho r_o^2}\frac{\partial r_o}{\partial z} \tag{9}$$

Now define $J = Q_{down}/H_{eff}$, noting that for a stationary foam Q_{down} is identical with $Q^o_{net\ down,SO}$ since $v_{b,MO} = v_{f,SO} = 0$. Combining the

aforesaid Equations (3), (6) and (9) with Equations 12, 14 and 22 of reference (2) with subscript "net down" replacing "net up", and also combining with $\hat{P} = 1$ and the definitions of J, Z, $\hat{q}$, $\hat{A}$, R, and X, yields Equation (10).

$$\hat{q} = J\left[\frac{BR^4}{1+ER^2} - CR^2\frac{\partial R}{\partial X}\right] \tag{10}$$

where $$B = \frac{P_o(A_{PB})_o^2 \rho g}{\mu q_o} \tag{11}$$

and $$C = \frac{\gamma P(A_{PB})_o^2}{\mu q_o L(r_o)_o} \tag{12}$$

From Equation (3)

$$\frac{\partial \hat{A}}{\partial \hat{T}} = 2R\frac{\partial R}{\partial \hat{T}} \tag{13}$$

Partially differentiating Equation (10) with respect to X, and combining with Equations(8) and (13), yields

$$\frac{1}{2}\left[\frac{BR^3}{1+ER^2} - CR\frac{\partial R}{\partial X}\right]\frac{\partial J}{\partial X} + \frac{J}{2}\left[\frac{4BR^2+2BER^4}{(1+ER^2)^2}\frac{\partial R}{\partial X} - 2C\left(\frac{\partial R}{\partial X}\right)^2 - CR\frac{\partial^2 R}{\partial X^2}\right] = -\frac{\partial R}{\partial \hat{T}} \tag{14}$$

J can be determined from its definition together with Figures 3 and 8 of reference (2). Over the range of current interest, J is very nearly a linear function of M. Thus,

$$J = k_1(M+k_2) \tag{15}$$

with $k_1 = 0.017$ and $k_2 = 0.0069$ here.

Since $R = M/M_o$,

$$J = k_1(M_oR + k_2) \tag{16}$$

Differentiating,

$$\frac{\partial J}{\partial X} = k_1 M_o \frac{\partial R}{\partial X} \qquad (17)$$

Combining Equations 14, 16, and 17, yields the final differential equation:

$$\frac{k_1}{2}\left[\frac{BR^2(3M_oER^3+2k_2ER^2+5M_oR+4k_2)}{(1+ER^2)^2}\frac{\partial R}{\partial X} - C(3M_oR+k_2)\left(\frac{\partial R}{\partial X}\right)^2 - CR(M_oR+k_2)\frac{\partial^2 R}{\partial X^2}\right] = -\frac{\partial R}{\partial \hat{T}} \qquad (18)$$

The boundary conditions are $R \simeq 0$ for $X = 0$ at all $\hat{T} > 0$, and $R = 1$ for $\hat{T} = 0$ at all $x > 0$. The first condition was closely approached by taking $R = 10^{-3}$. (Employing in turn 10^{-4}, 10^{-2}, and 10^{-1} yielded no significant difference.) To facilitate solution, another boundary condition was employed, namely $\frac{\partial R}{\partial X} = 0$ at $X = 0$ for all $\hat{T}$. This is valid for the early density history of a point high up the foam column, and approximate thereafter.

SOLUTION AND COMPARISON

Approximating differentials with finite differences of lowest order yields Equation (19) as the finite difference replacement for Equation (18).

$$\frac{k_1}{2}\left[\frac{BR_i^2}{1+ER_i^2}\left(\frac{3M_oER_i^3+2k_2ER_i^2+5M_oR_i+4k_2}{1+ER_i^2}\right)\left(\frac{R_i-R_{i-1}}{\Delta X}\right) - C(3M_oR_i+k_2)\left(\frac{R_i^2-2R_{i-1}R_i+R_{i-1}^2}{(\Delta X)^2}\right) - CR_i(M_oR_i+k_2)\left(\frac{R_{i+1}-2R_i+R_{i-1}}{(\Delta X)^2}\right)\right]_{t-1} = -\left(\frac{R_t-R_{t-1}}{\Delta \hat{T}}\right) \qquad (19)$$

$R_t - R_{t-1}$ is of course the change in R over the time interval $\Delta\tau$.

The final boundary condition becomes, via a four term Taylor series expansion, the following:

$$\frac{k_1 C R_1 (M_o R_1 + k_2)}{2} \left(\frac{-R_{i-2} + 8R_{i-1} - 7R_i}{2(\Delta X)^2} \right) \Bigg|_{t-1} = \frac{R_t - R_{t-1}}{\Delta \hat{T}} \qquad (20)$$

The difference equations were solved by stepwise procedure with an I.B.M. 1620 digital computer.

As of this writing, only one experimental run has been compared against, and at only one level in the foam, namely 70 cm. up a 120 cm. column. The experimental variation in foam density with time was measured via electrical conductivity using the same apparatus described in reference (1) which accompanies the present Progress Report.

Figure 4 shows the comparison between the theoretical curve and the experimental curve. The importance of coalescence in the foam is immediately evident. The theoretical curve makes no allowance for it. Its actual effect is to internally feed additional liquid on to the 70 cm. level from the coalescence above it, thus preventing the density at that level from falling as rapidly at first as it might otherwise. Later, when coalescence becomes prominent at the 70 cm. level itself, the destruction of capillaries (Plateau borders) makes for a more rapid fall in density than would be the case without such coalescence.

Besides showing the importance of coalescence, the aforementioned comparison gives a measure (by difference) of its extent.

Further work on the subject of coalescence is planned.

Privileged Communication

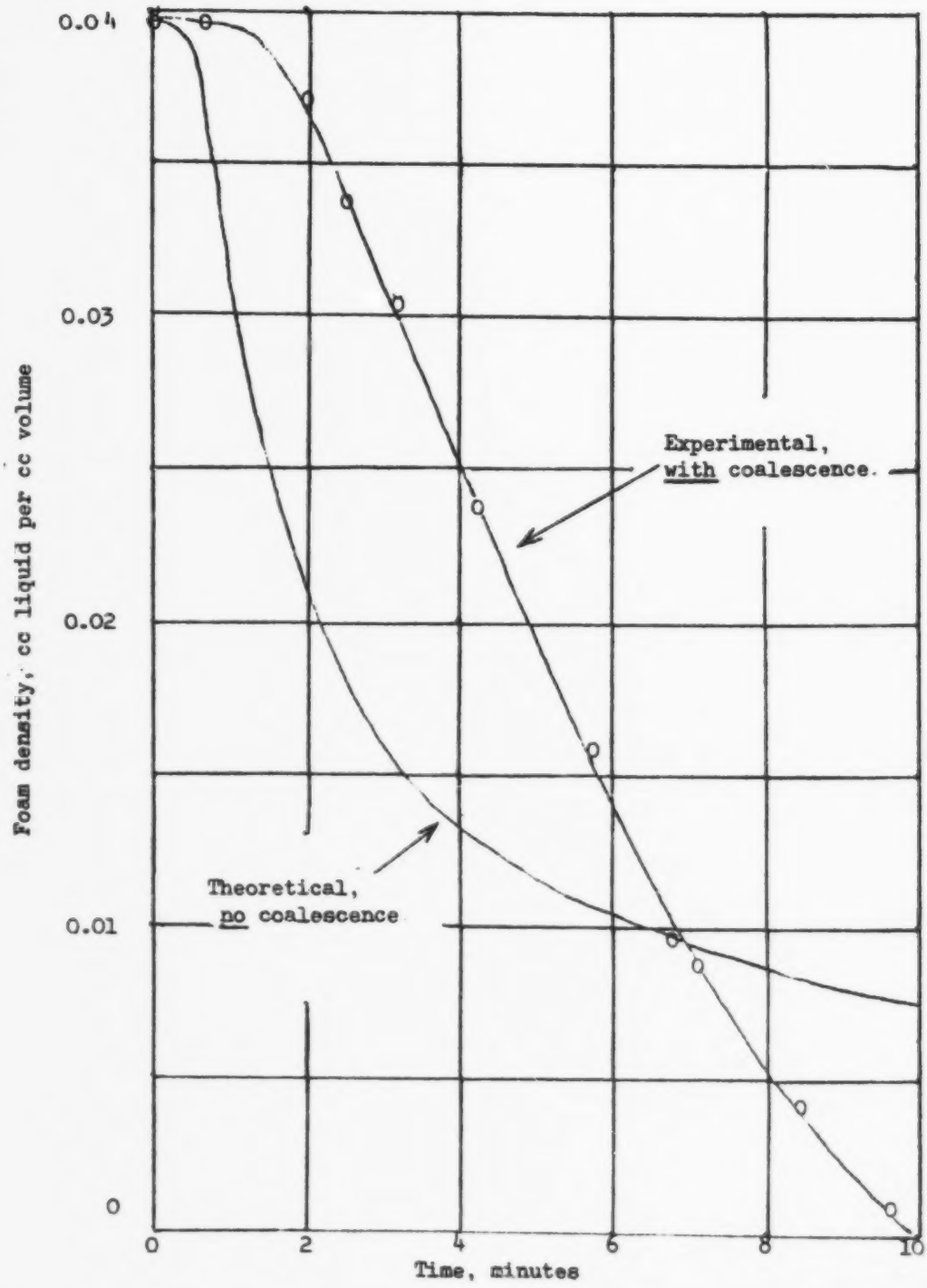

Figure 4. Typical density history at a particular level in a stationary foam draining at unsteady state.

LITERATURE CITED

1. Fanlo, S. and Lemlich, R., A.I.Ch.E.-I.Chem.E. Symposium Series (London: Instn.Chem.Engrs.) No. 9, 75 (1965).

2. Leonard, R. A. and Lemlich, R., Am.Inst.Chem.Engrs. Jour. 11:18 (1965).

3. _____ and _____, ibid. 11:25 (1965).

4. Shih, F. S. and Lemlich, R., ibid., in review.